

# *AGN 研究の進展*

梅村 雅之

筑波大学 計算科学研究セン

理論天文学懇談会シンポジウム2006(立教大学)

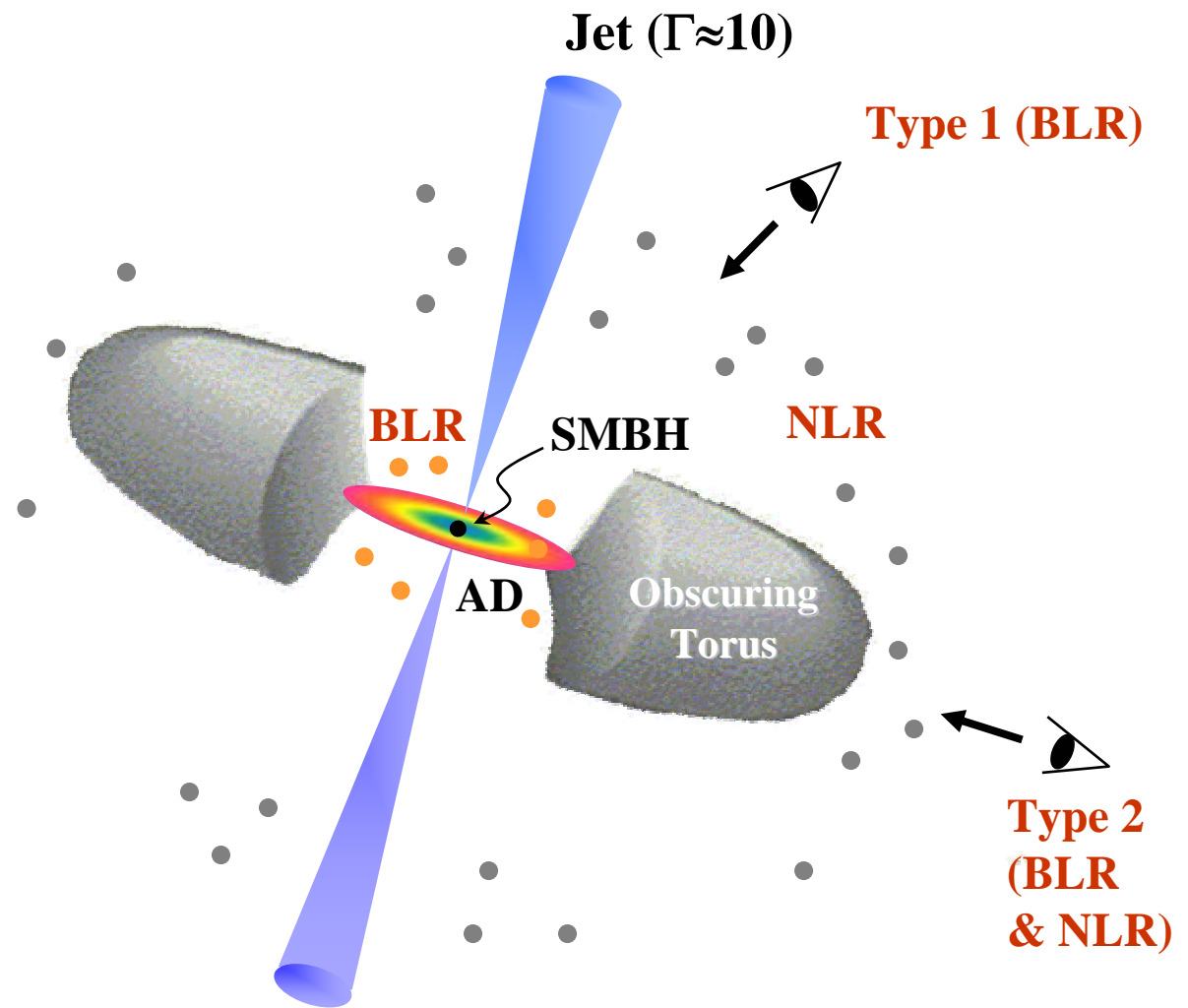
# AGN GUT

## 30年来のパラダイム

超巨大ブラックホール  
(SMBH)

降着円盤  
(AD)

遮蔽トーラス  
(Obscuring Torus)



BLR: Broad Line Regions, NLR: Narrow Line Regions

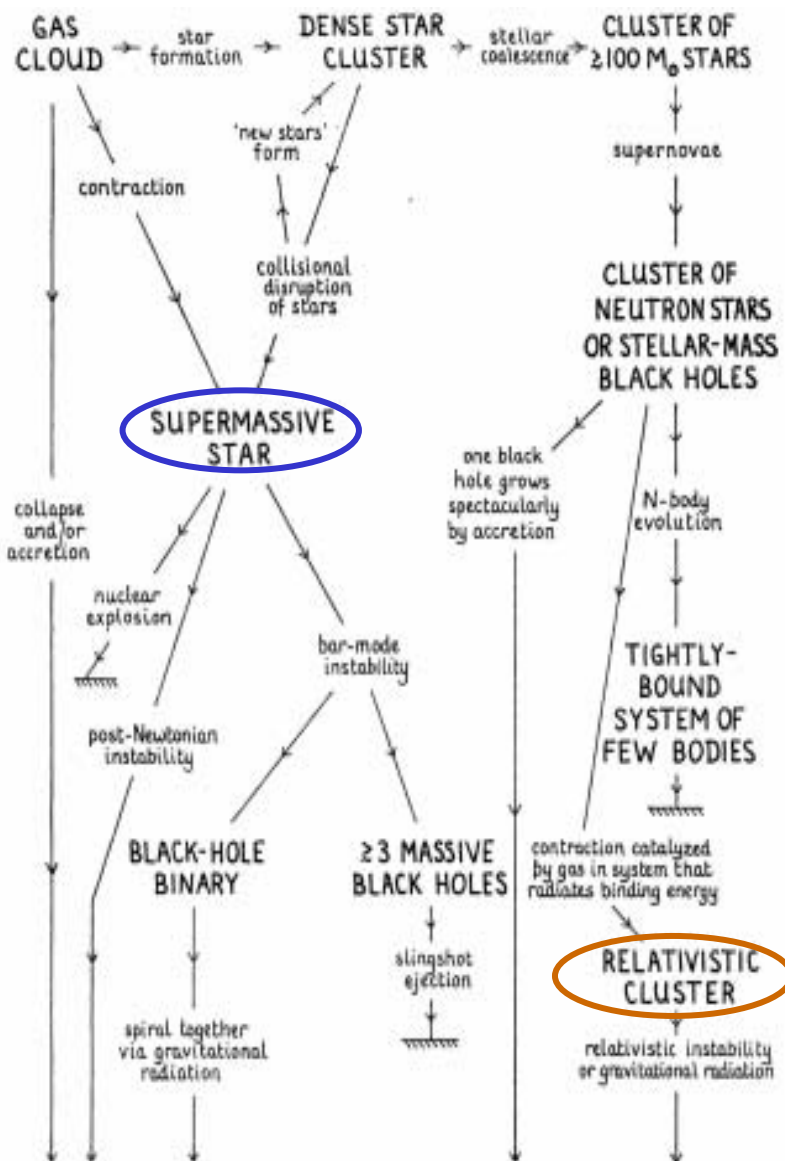
# **Part 1 超巨大ブラックホール形成**

# Rees Diagram (1984)

Supermassive Star ?

or

Cluster ?



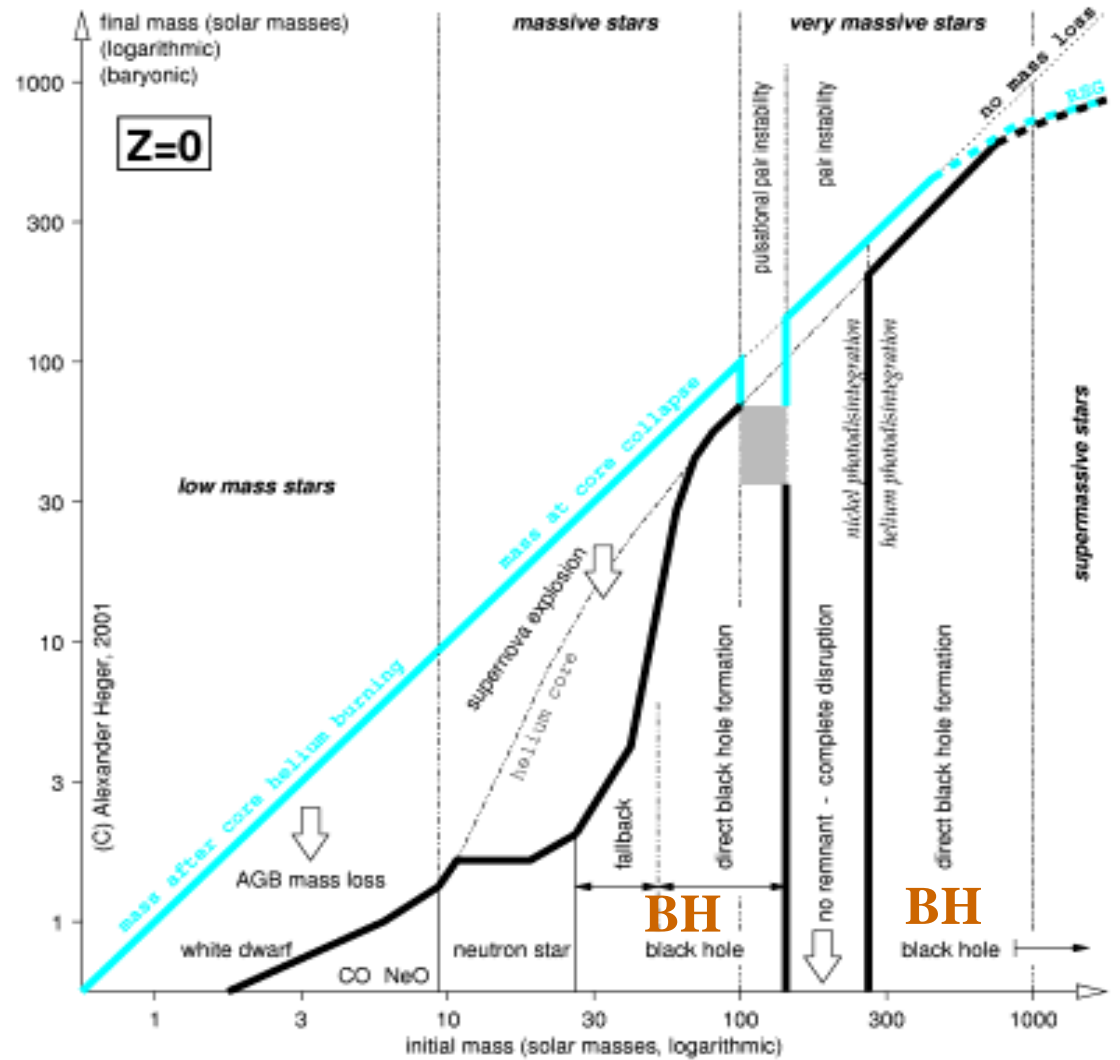
**massive black hole**

Figure 1 Schematic diagram [reproduced from Rees (106)] showing possible routes for runaway evolution in active galactic nuclei.

# Seed BHs

## Pop III Stars

Heger & Woosley 2002,  
ApJ, 567, 532



# Supermassive Star

## General Relativistic Instability

Rapidly rotating supermassive star  
in equilibrium



- rigid rotation
- mass-shedding limit
- unstable at

$$R < 640GM/c^2$$

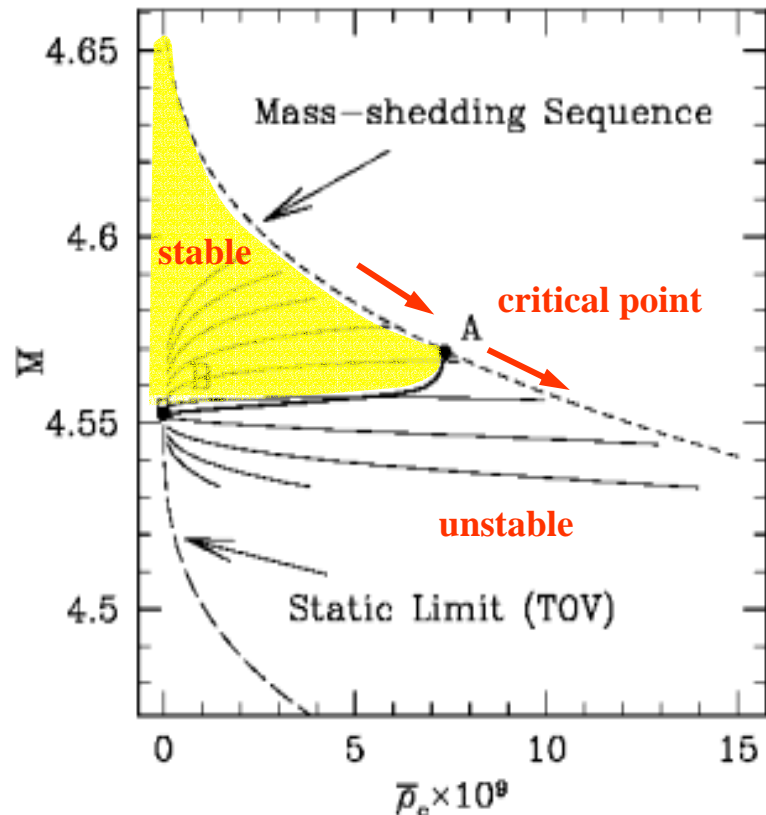


FIG. 2.—Mass vs. central density plot for relativistic, rotating  $n = 3$  polytropes. The long-dashed curve is the Tolman-Oppenheimer-Volkoff (TOV) solution for nonrotating, static configurations, and the short-dashed curve marks the mass-shedding limit. The thin solid lines denote sequences of constant angular momentum, ranging from  $J = 15$  (lowest curve) to  $J = 24$  (highest curve) in increments of  $\Delta J = 1$ . Turning points of these curves mark the onset of instability. The thick solid line connects these turning points (see also Fig. 3) and hence separates a region of stable configurations (*above this line*) from a region of unstable configurations (*below this line*). In particular, all nonrotating  $n = 3$  polytropes are unstable to radial perturbations. A configuration evolving along the mass-shedding sequence with increasing central density becomes unstable at the critical point A. All sequences of constant angular momentum connect the mass-shedding limit with point B for  $\rho_c \rightarrow 0$  (and hence  $R \rightarrow \infty$ ). The mass of this configuration should agree with the mass  $M = 4.5525$  of a Newtonian  $n = 3$  polytrope (eq. [26]; *open circle*). The deviation of the solid point B from the analytical value is a measure of our numerical accuracy.

Baumgarthe & Shapiro 1999, ApJ, 526, 941

# Dynamical Collapse (Post Newtonian)

Saijo, Shibata, Baumgarte, & Shapiro  
(2001, ApJ, 548, 919)

Differentially rotating SMS  
⇒ bar instability

Saijo, Baumgarte, Shapiro & Shibata  
(2002, ApJ, 569, 349)

Rigid rotating SMS  
⇒ collapse

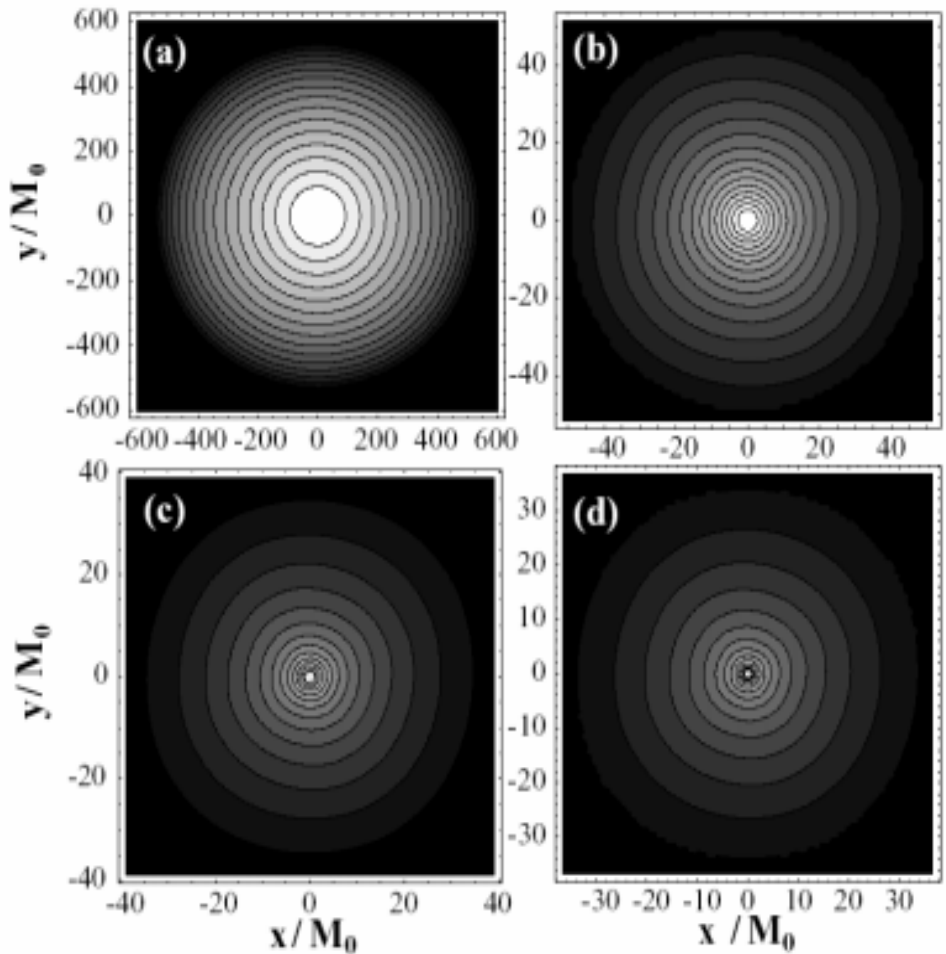


FIG. 14.— Density contours  $\rho_*$  in the equatorial plane at selected times during rotating SMS collapse. Snapshots are plotted at  $(t/t_{\Gamma}, d) =$  (a)  $(5.0628 \times 10^{-4}, 8.254 \times 10^{-9}, 10^{-7})$ , (b)  $(2.50259, 1.225 \times 10^{-4}, 10^{-5})$ , (c)  $(2.05360, 8.328 \times 10^{-3}, 5.585 \times 10^{-7})$ , (d)  $(2.5425 \times 10^{-2}, 1.357 \times 10^{-7})$ , respectively. The contour lines denote densities  $\rho^* = \rho_c^* \times d^{(1-4/16)}$  ( $i = 1, \dots, 15$ ).

# Dynamical Collapse (Full General Relativity)

Shibata & Shapiro 2002, ApJ, 572, L39

Dynamical collapse  $\Rightarrow$  Apparent Horizon

Kerr parameter  $\bullet$  0.75 (Kerr BH)

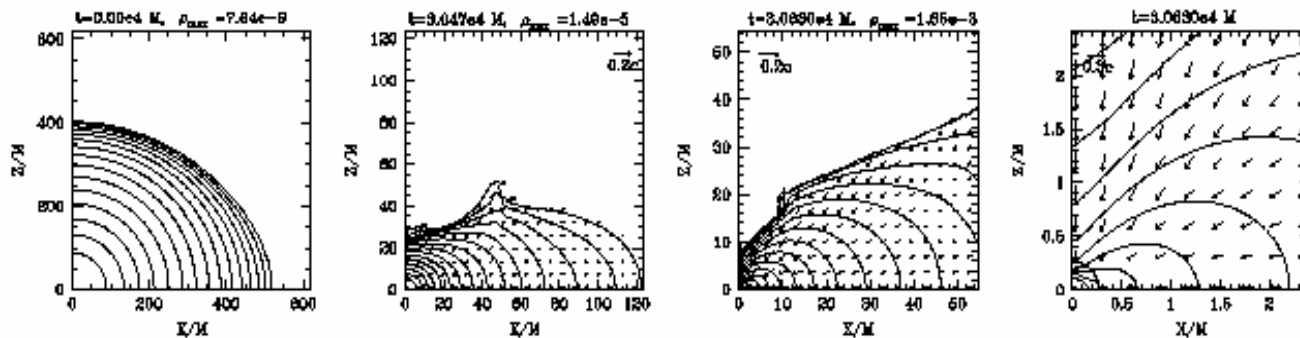


FIG. 1.— Snapshots of density contour lines and velocity vectors in the  $x$ - $z$  plane at selected time slices. The contour lines are drawn for  $\rho/\rho_{\max} = 10^{-0.4j}$  ( $j = 0 \sim 15$ ), where  $\rho_{\max}$  denotes the maximum density. The fourth figure is the magnification of the third one: The thick solid curve at  $r \approx 0.3M$  denotes the location of the apparent horizon.

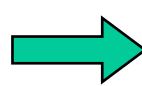
Supermassive star (rigidly rotating)  $M \gtrsim 10^6 M_\odot$

$$\downarrow \quad R < 640 GM/c^2$$

General relativistic instability (Baumgarte & Shapiro 1999, ApJ, 526, 941)



Dynamical collapse  
(Post Newtonian)



Apparent horizon  
(Full GR)

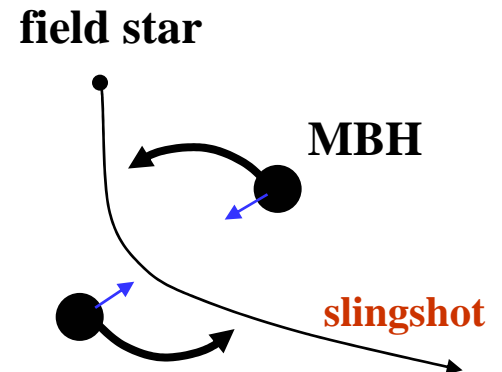
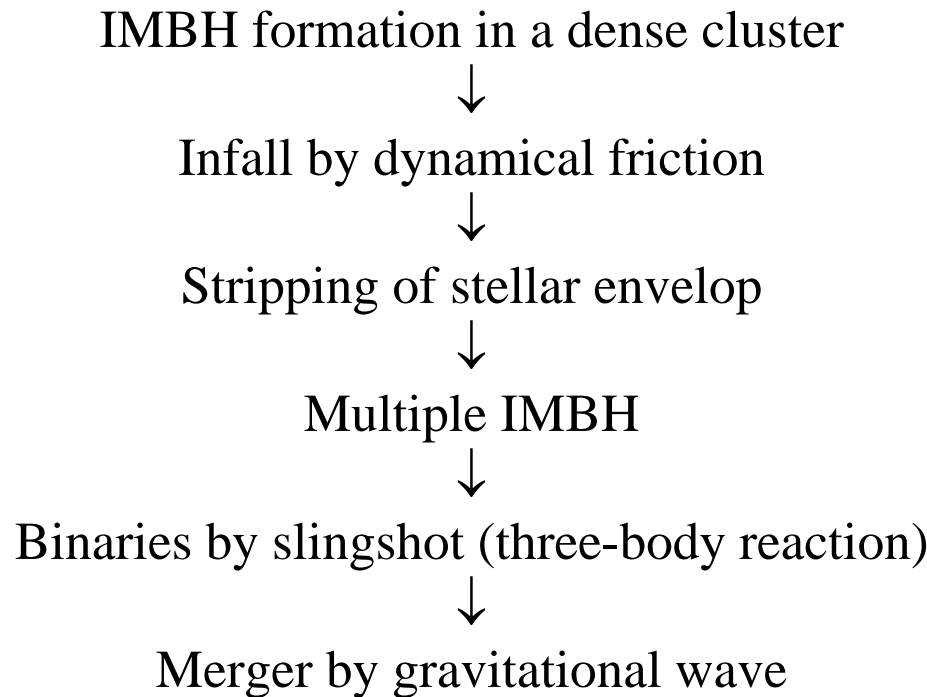
(Saijyo, Baumgarte, Shapiro  
& Shibata 2002, ApJ, 569, 349)

Kerr BH with spin parameter of 0.75  
(Shibata & Shapiro 2002, ApJ, 572, L39)

# Mechanisms due to N-Body Process

Dynamical Friction (Makino 2002)

$$t_{\text{fric}} ; \frac{1.17}{\log \Lambda} \frac{r^2 v_c}{Gm} = 6 \times 10^8 \text{ yr} \left( \frac{r}{\text{kpc}} \right)^2 \left( \frac{v_c}{100 \text{ km s}^{-1}} \right) \left( \frac{m}{5 \times 10^6 M_\odot} \right)^{-1}$$



(1) Dynamical Friction  
effective at  $M_{\text{BH}} < M_*$

$$\rho_* \propto r^{-2} \quad (M_* \propto r)$$

$$M_* = 10^6 M_\odot \left( \frac{r}{0.1 \text{pc}} \right) \left( \frac{M_{\text{gal}}}{10^{10} M_\odot} \right) \left( \frac{R_{\text{gal}}}{1 \text{kpc}} \right)$$

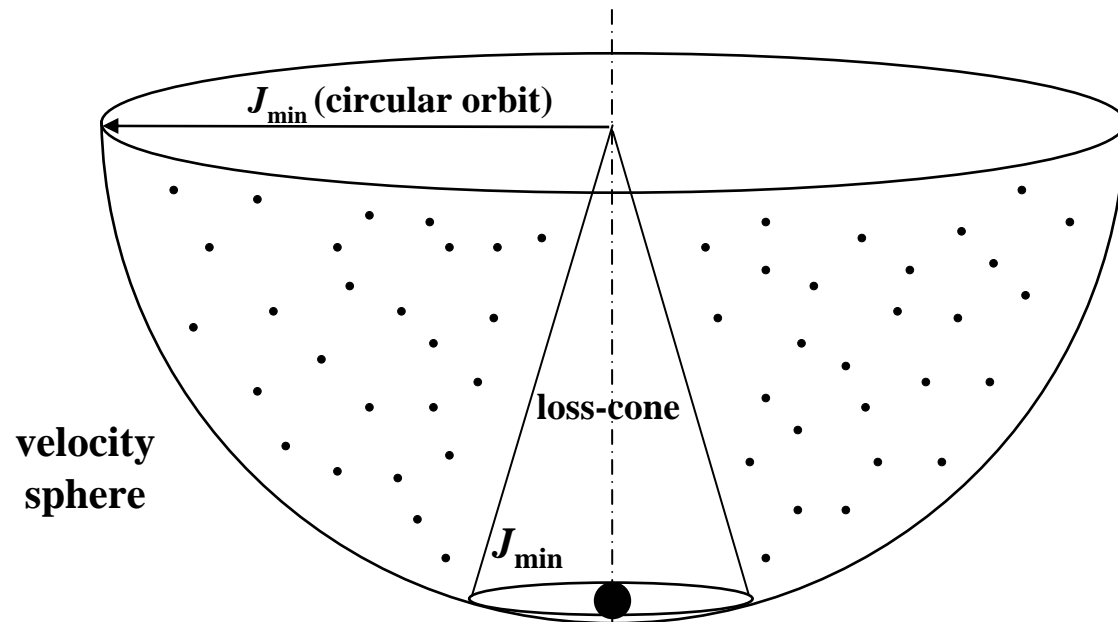
(2) Gravitational wave

$$t_{GW} ; \frac{r}{c} \left( \frac{r}{r_g} \right)^3 = 2 \times 10^{18} \text{yr} \left( \frac{r}{0.1 \text{pc}} \right)^4 \left( \frac{M_{\text{BH}}}{10^6 M_\odot} \right)^{-3}$$

(3) Loss-cone depletion by slingshot

# Loss-cone Depletion in Binary

Begelman, Blandford, Rees, 1980, Nature, 287, 307



ejection by slingshot

# Loss-cone Depletion in MBH Binary

Makino & Funato, 2004, ApJ, 602, 93

MBH binaryは, slingshotによるhardeningでは,  
Hubble time 内に重力波放出の軌道まで縮まらない

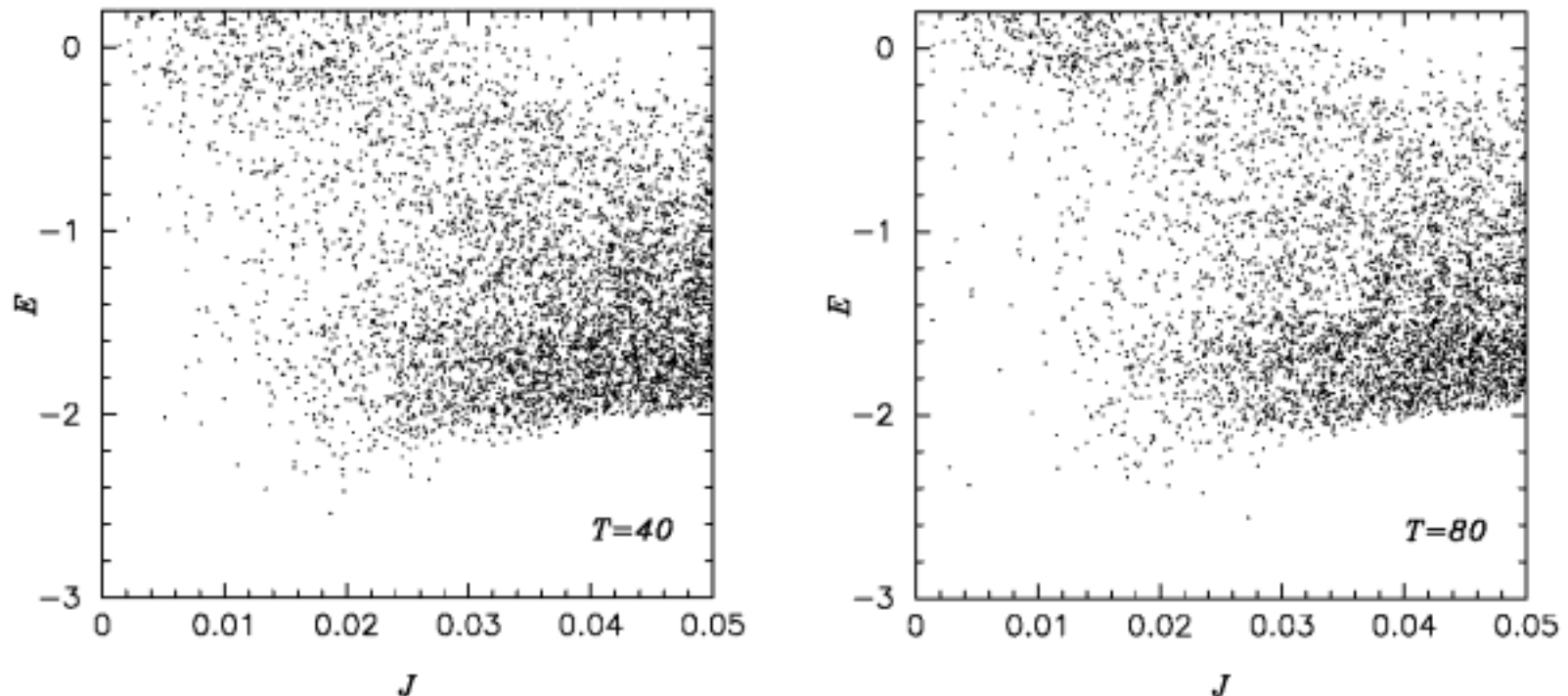
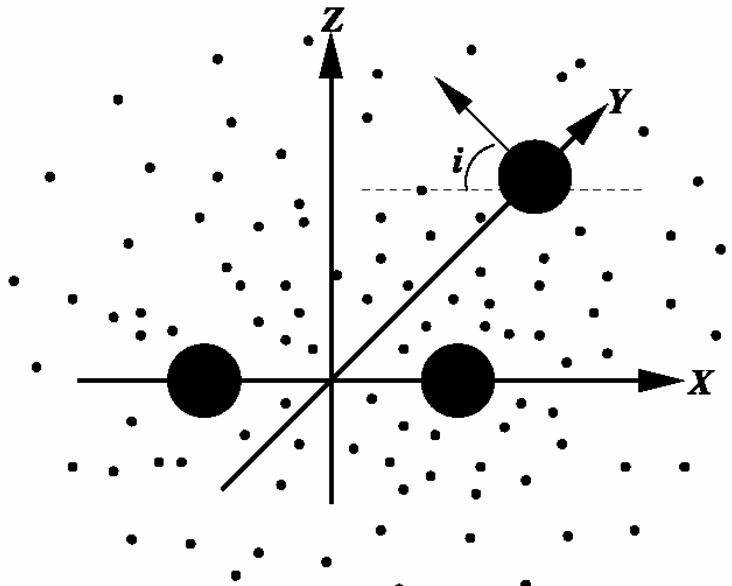


Fig. 8.—Distribution of particles in the  $(E, J)$  plane at times  $T = 10, 20, 40$  and  $80$  (top left to bottom right). The number of particles is  $10^6$ .

# MBH Triplet

Iwasawa, Funato, & Makino, 2006, ApJ, 651, 1059

Eccentricity の大きい BH binary は, single BH との  
3体相互作用で重力波放出の軌道まで縮まる



High eccentricity BH binary 形成

強3体相互作用による eccentricity  
thermalization

Kozai メカニズムによる 経年的変化



多くの MBH は, binary として残る

# 超巨大BH - 銀河バルジ関係

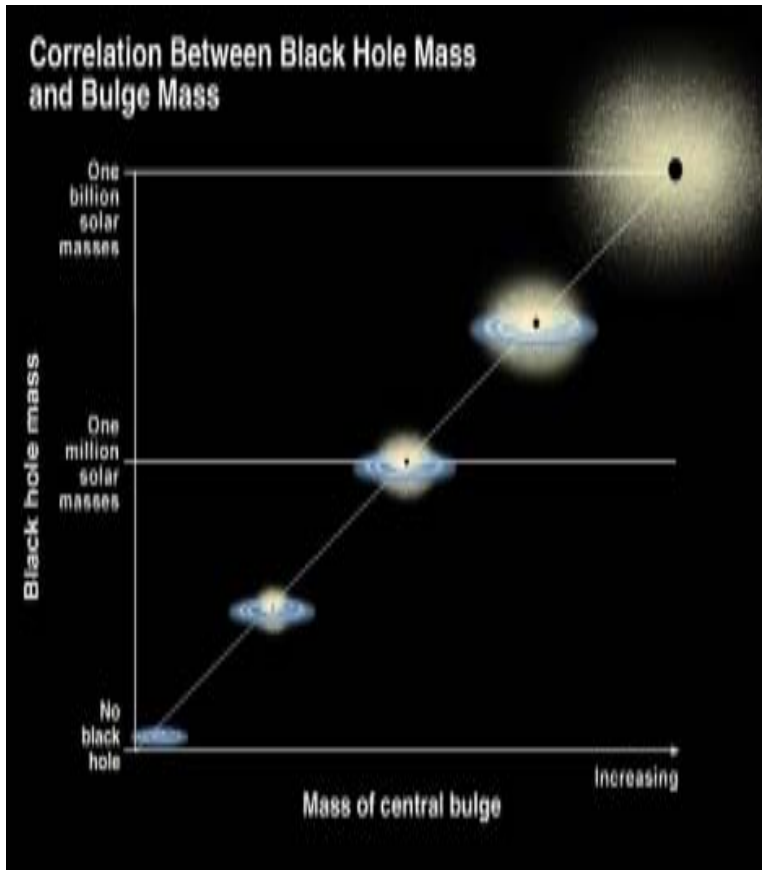
$$M_{\text{BH}} / M_{\text{bulge}} \approx 0.001$$

Kormendy & Richstone 1995

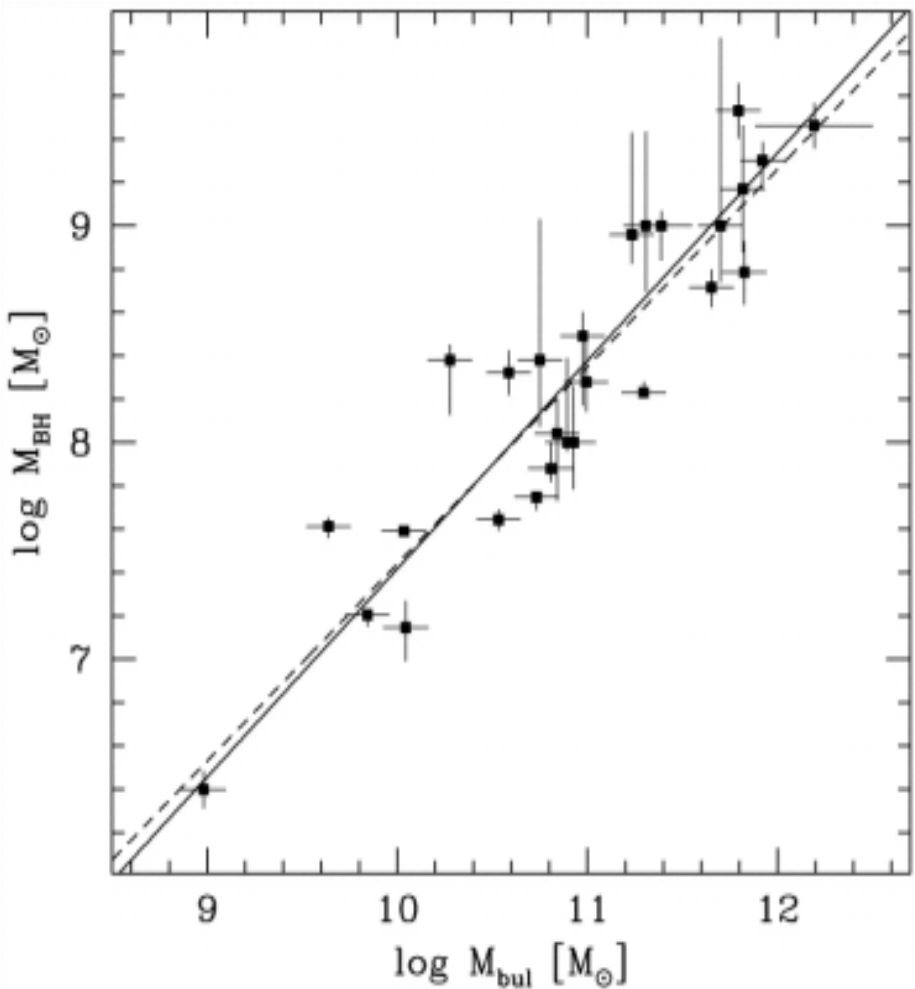
Magorrian et al. 1998

Merritt & Ferrarese 2001

Marconi & Hunt 2003



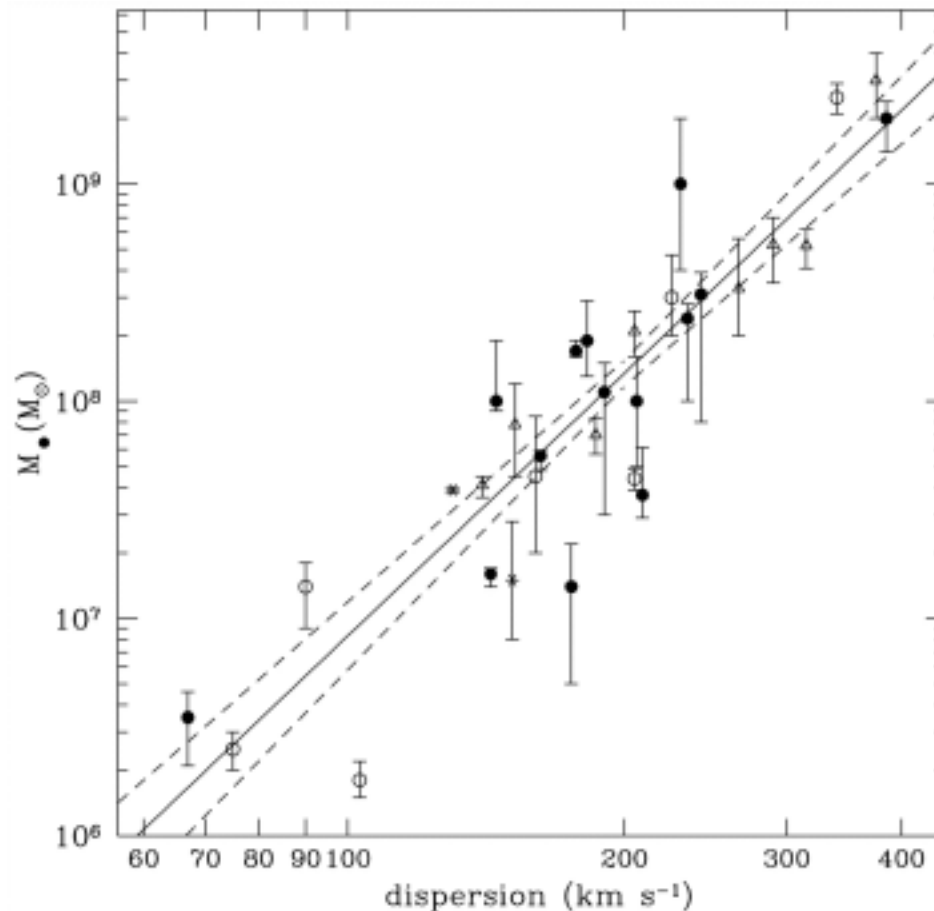
Marconi & Hunt 2003, ApJ, 589, 21



# $M_{\text{BH}}$ - $\sigma$ Relation

$$M_{\text{BH}} \approx 10^8 M_{\odot} \left( \frac{\sigma}{200 \text{km/s}} \right)^4$$

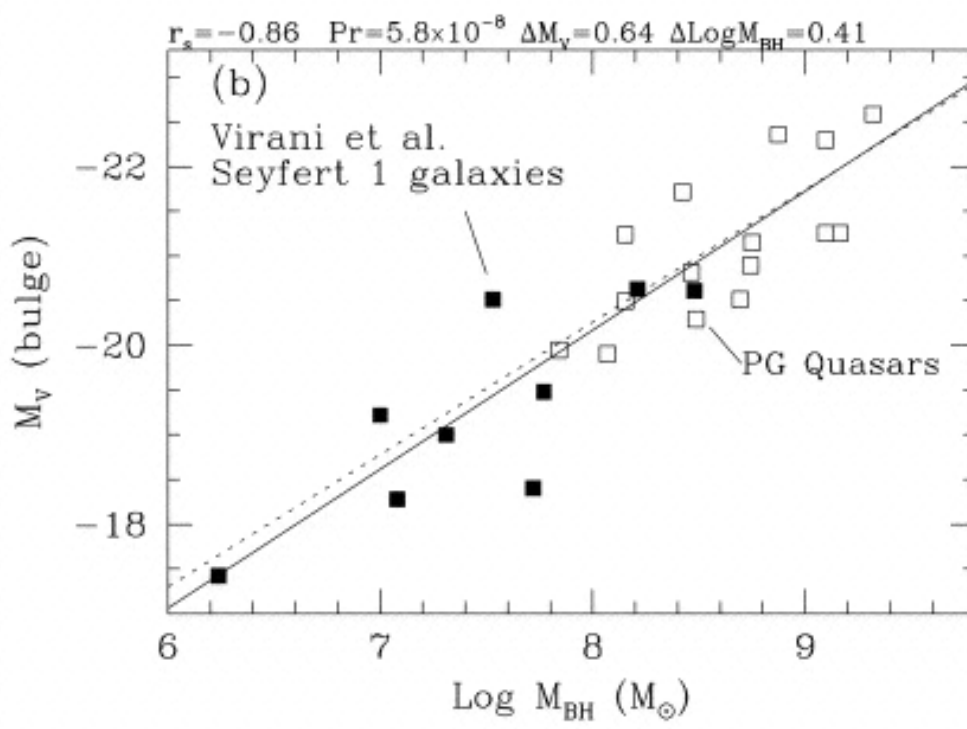
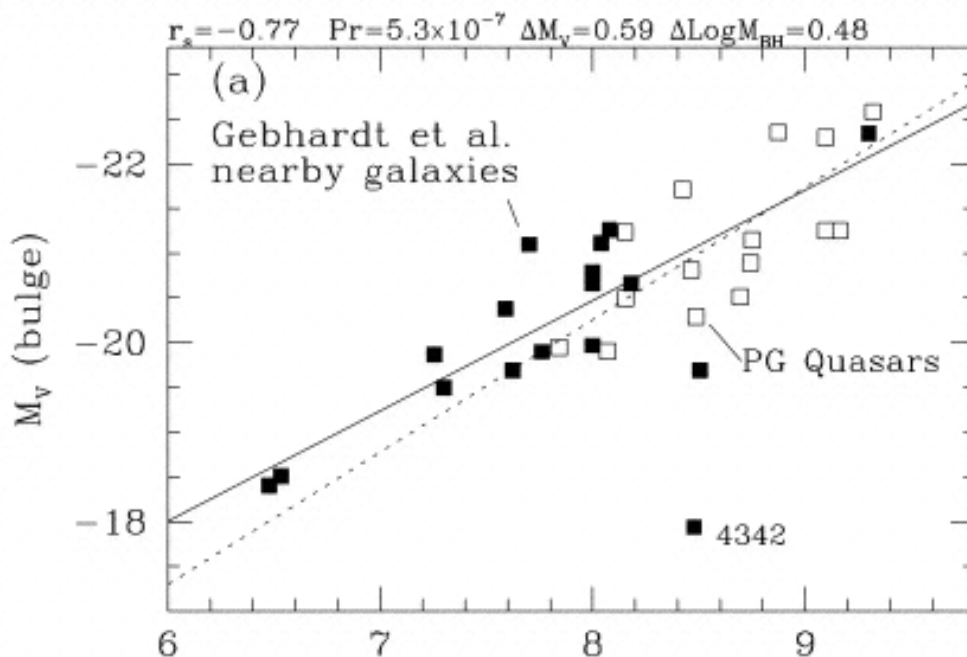
σ: バルジの速度分散



Tremaine et al. 2002, ApJ, 574, 740

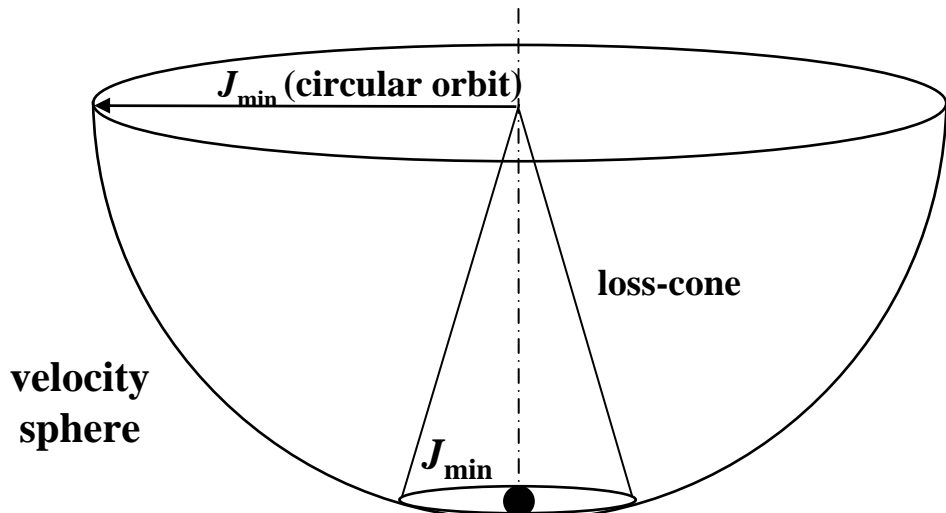
# クエーサー

Laor 2001, ApJ, 553, 677



# Direct Capture of Stars

Adams et al. 2003, ApJ, 591, 125



**stellar density**

$$\rho = \frac{\sigma_v^2}{4\pi G r^2}, \quad M(r) = \frac{\sigma_v^2}{G} r$$

$$r_p = \frac{j^2}{2GM_{\text{BH}}} = \frac{(GM_{\text{BH}})^3 \Omega^2}{2\sigma_v^4}$$

**spin parameter**

$$\lambda = \frac{J |E|^{1/2}}{GM^{5/2}} = 0.035$$

**direct capture**

$$r_p < 4r_s$$

$$\Rightarrow M_{\text{BH}} = \frac{4\sigma_v^4}{Gc\Omega} \approx 10^8 M_{\odot} \left( \frac{\sigma_v}{200 \text{ km/s}} \right)^4$$

# Tidal Disruption & Capture of Star by SMBH

Tidal disruption radius

$$\frac{GM_{BH}M_\odot}{r_{disr}^3} = \frac{GM_\odot}{R_\odot^2} \Rightarrow r_{disr} = R_\odot \left( \frac{M_{BH}}{M_\odot} \right)^{1/3}$$

Direct capture

$$J \leq \frac{4GM_{BH}}{c}$$

$$r_{disr} < r_s \Rightarrow r_{disr} = \left( \frac{M_{BH}}{10^8 M_\odot} \right)^{-2/3} r_s$$

10<sup>8</sup>M<sub>○</sub>以上のBHでは，星は潮汐破壊の前にBH horizonに吸い込まれる  
←  
輻射を出さない(AGNにならない)

# QSO Luminosity Functionからの制限

## Integration of QSO LF

$$\Omega_{\text{BH}}(\text{QSO}) \approx 1.8 \times 10^{-6}$$

Yu & Tremaine 2002, MNRAS, 335, 965

$$\Omega_{\text{BH}}(\text{QSO}) \approx (2.4 - 4.8) \times 10^{-6}$$

Marconi et al. 2004, MNRAS, 351, 169

## SMBH-bulge mass relation at z=0

$$\Omega_{\text{BH}}(\text{bulge}) \approx 2.1 \times 10^{-6}$$



QSO BHの最終フェーズはガスアクリーションで太った

# Relativistic Radiation Hydrodynamics

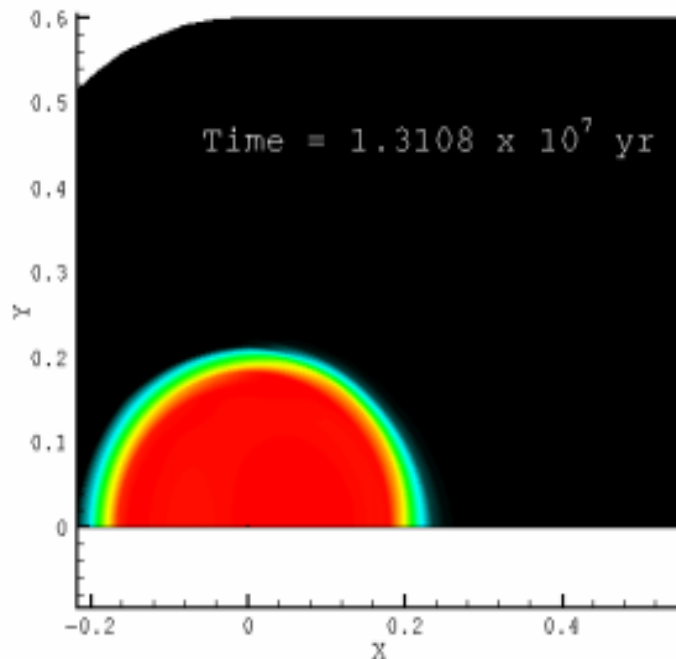
Equation of motion  $O(v/c)$

$$\rho \frac{d\mathbf{v}}{dt} = \mathbf{f} - \nabla p + \frac{1}{c} (\kappa_0 + \sigma_0) [\mathbf{F} - (E + \mathbf{P})\mathbf{v}]$$

absorption  
scattering

Radiation drag

e.g. Poynting-Robertson effect  
in solar system



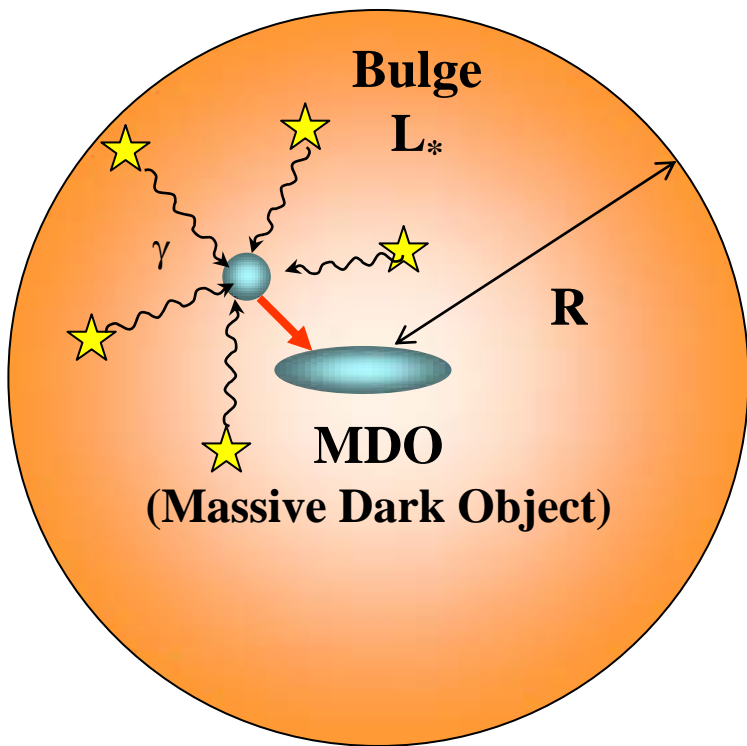
Sato, MU, Sawada, Matsuyama,  
2004, MNRAS, 354, 176

# SMBH Formation by Radiation Drag in Bulge

Umemura, 2001, ApJ, 560, L29

Kawakatsu & Umemura, 2002, MNRAS, 329, 572

## Angular Momentum Extraction



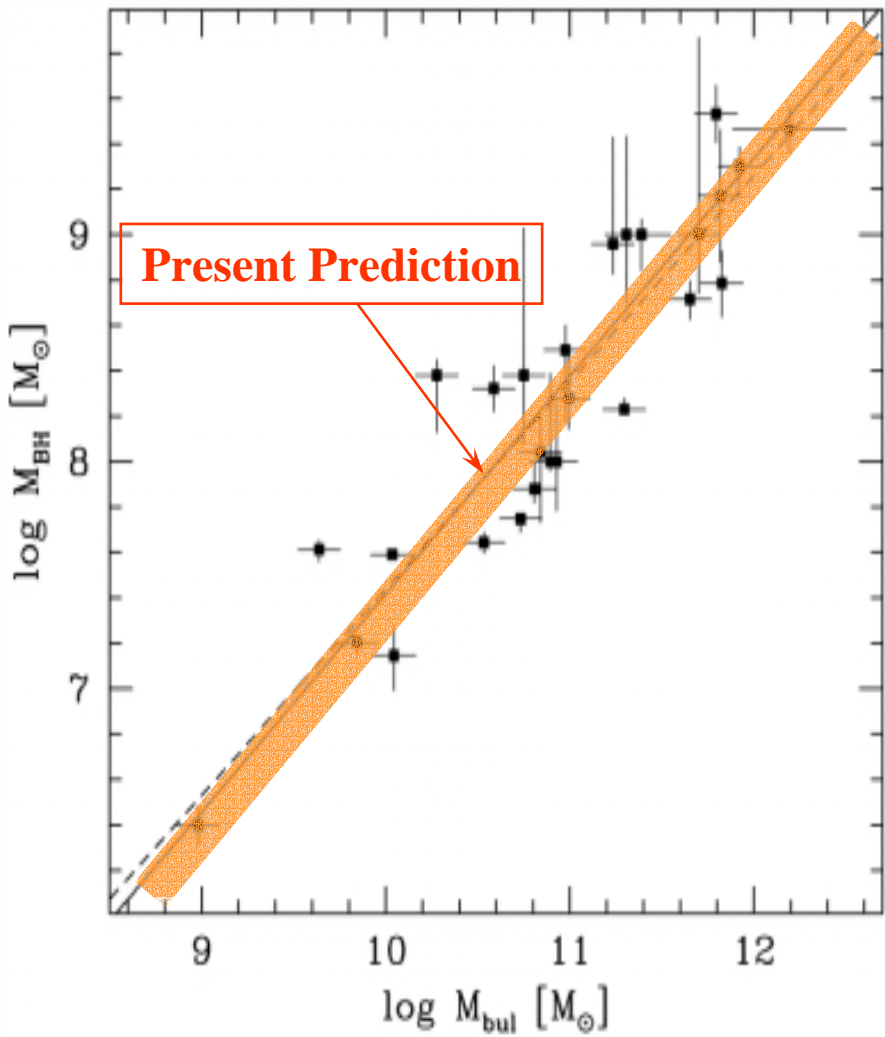
## *Poynting-Robertson Effect*

$$\frac{d \ln J}{dt} ; -\frac{\chi E}{c} ; -\frac{\chi L_*}{c^2 R^2} = -\frac{L_*}{c^2 M_g} (1 - e^{-\tau})$$

( $\tau$ : optical depth by dust) photon number conservation

## Mass Accretion Rate

$$\dot{M} \equiv -M_g \frac{d \ln J}{dt} ; \frac{L_*}{c^2} (1 - e^{-\tau})$$



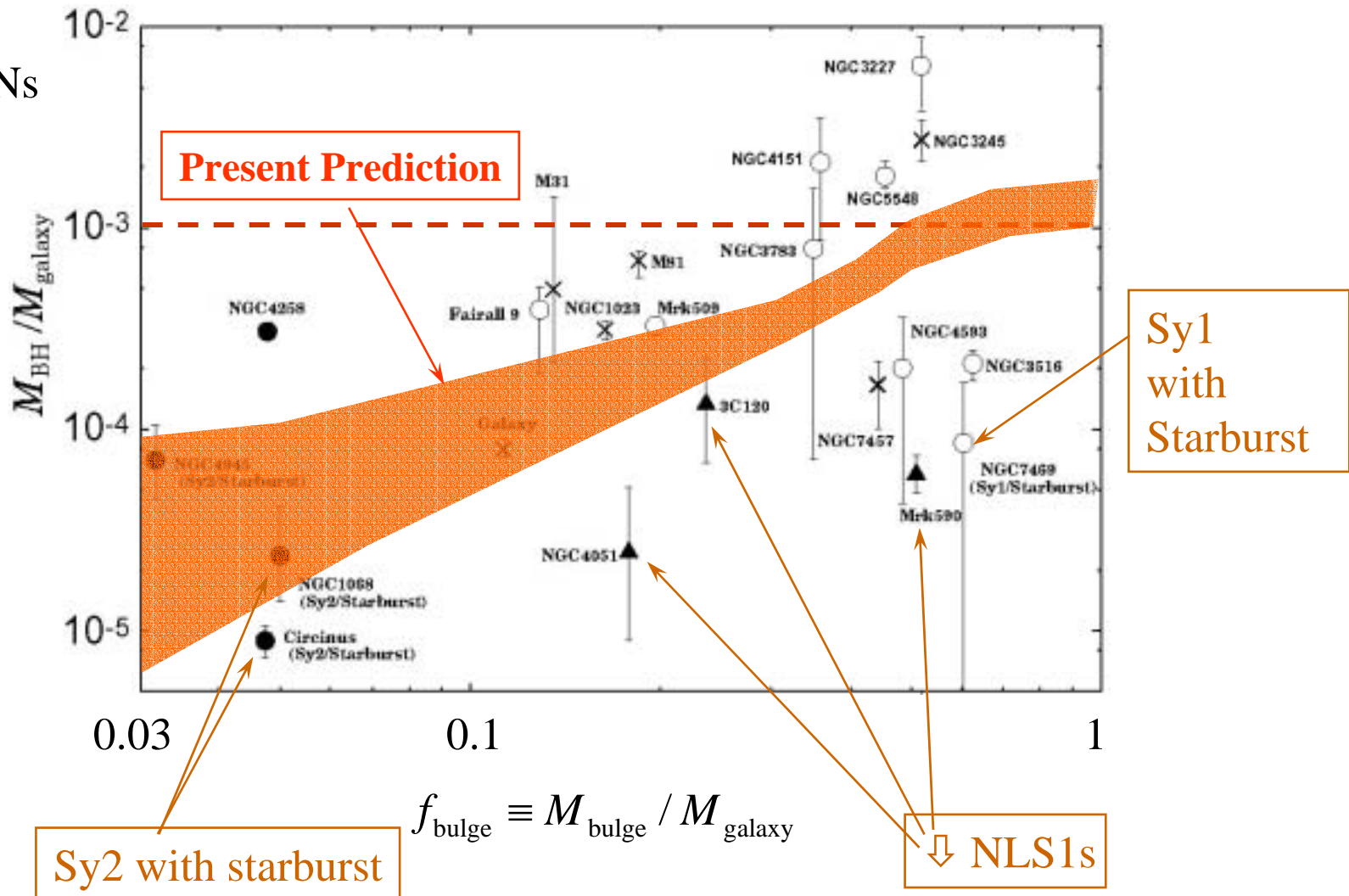
$$\frac{M_{\text{BH}}}{M_{\text{bulge}}} ; \quad 0.14\varepsilon = 0.001$$

$\varepsilon = 0.007$  : Hydrogen burning energy conversion efficiency

$$(e_{\text{rad}} = l_* t_* ; \quad 0.14\varepsilon \cdot m_* c^2)$$

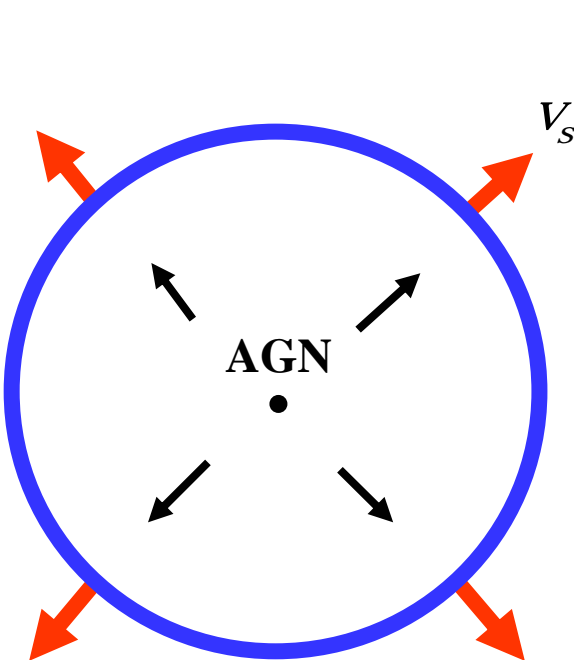
# Why small BHs in disks?

- × Disks without AGNs
- ← Sy1s
- ↓ Sy2s
- ↓ NLSy1s



# AGN Feedback Regulation

Silk & Rees 1998, A&A, 331, L1



gas density

$$\rho = f_{\text{gas}} \frac{\sigma^2}{2\pi G r^2}, \quad M(r) = f_{\text{gas}} \frac{2\sigma^2}{G} r$$

velocity of expanding shell driven by AGN

$$v_s = \left( \frac{8\pi^2 G f_w L_E}{f_{\text{gas}} \sigma^2} \right)^{1/3}$$

feedback condition

$$v_s > \sigma \quad (= \sqrt{2}\sigma_v)$$

$$\Rightarrow M_{BH} = \frac{\sigma^5 \kappa}{G^2 c} \approx 10^8 M_\odot \left( \frac{\sigma_v}{200 \text{ km/s}} \right)^5$$

# Downsizing

## SMBH 大きなBHほど先にできた

Ueda et al. 2003, ApJ, 598, 886

Hasinger et al. 2003, astro-ph/0302574

Marconi et al. 2004, MNRAS, 351, 169

Merloni, 2004, MNRAS, 353, 1035

## Galaxies 大きな銀河ほど先に生まれた

Cowie et al. 1996, AJ, 112, 839

Kauffmann et al. 2003, MNRAS, 341 54

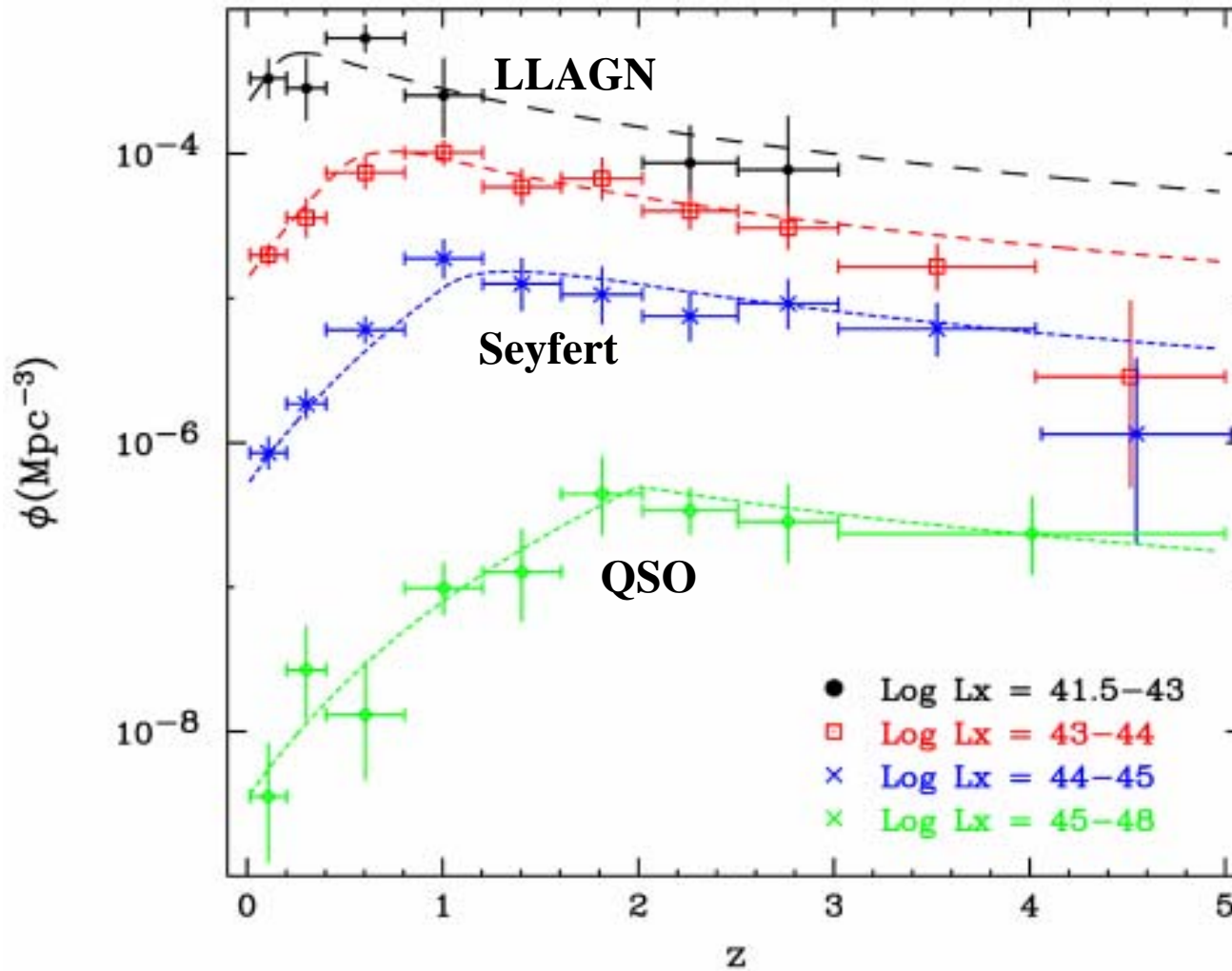
Kodama et al. 2004, MNRAS, 350, 1005

Glazebrook et al. 2004, Nature, 430, 181

# “Downsizing” in SMBH Formation

*More massive BHs formed at higher redshifts.*

Ueda et al. 2003, ApJ, 598, 886; Ueda et al. 2006



超巨大ブラックホールのダウンサイ징

+

SMBH-bulge 関係

||

重いバルジほど昔星形成を終了した

早期型銀河は早期に出来た

銀河と超巨大BHの共進化

# ブラックホール形成と成長

## 課題

Seed BH

$$M_{\text{BH}} = 1 - 10^5 M_{\odot}$$

SN/GRB remnant (Pop III remnant) ( $1-10^3 M_{\odot}$ )  
Supermassive star ( $10^{4-5} M_{\odot}$ )



ガス降着(Super/Sub-Eddington)  
合体成長  $t \approx 10^8$  yr

$$M_{\text{BH}} = 10^6 M_{\odot}$$

ガス降着  $t \approx 10^{7-9}$  yr

$$M_{\text{BH}} = 10^{8-9} M_{\odot}$$

銀河との共進化

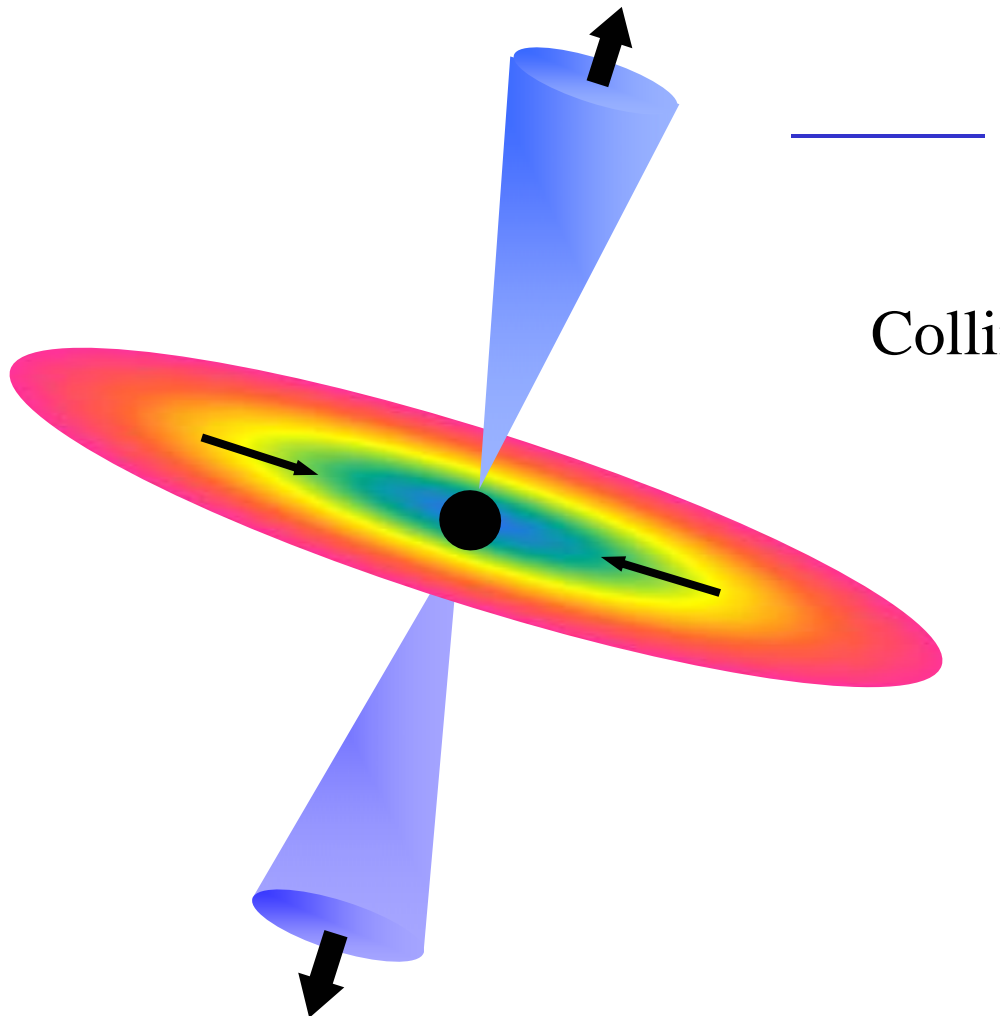
銀河スケールからサブパーセックへのアクリーション

## **Part 2 降着円盤 & ジェット**

# Accretion & Jet

降着円盤

角運動量輸送  
定常解



ジェット

加速メカニズム  
Collimation

## $\alpha$ -Prescription

viscosity coefficient  $\nu = \alpha C_s^2 \Omega^{-1}$

### 角運動量輸送

$$\frac{dJ}{dt} = -\frac{d}{dr} \left( \frac{\alpha C_s^2}{\Omega} r \frac{dv_\phi}{dr} \right) \quad (= -\frac{\alpha C_s^2}{2} \text{ for Kepler})$$

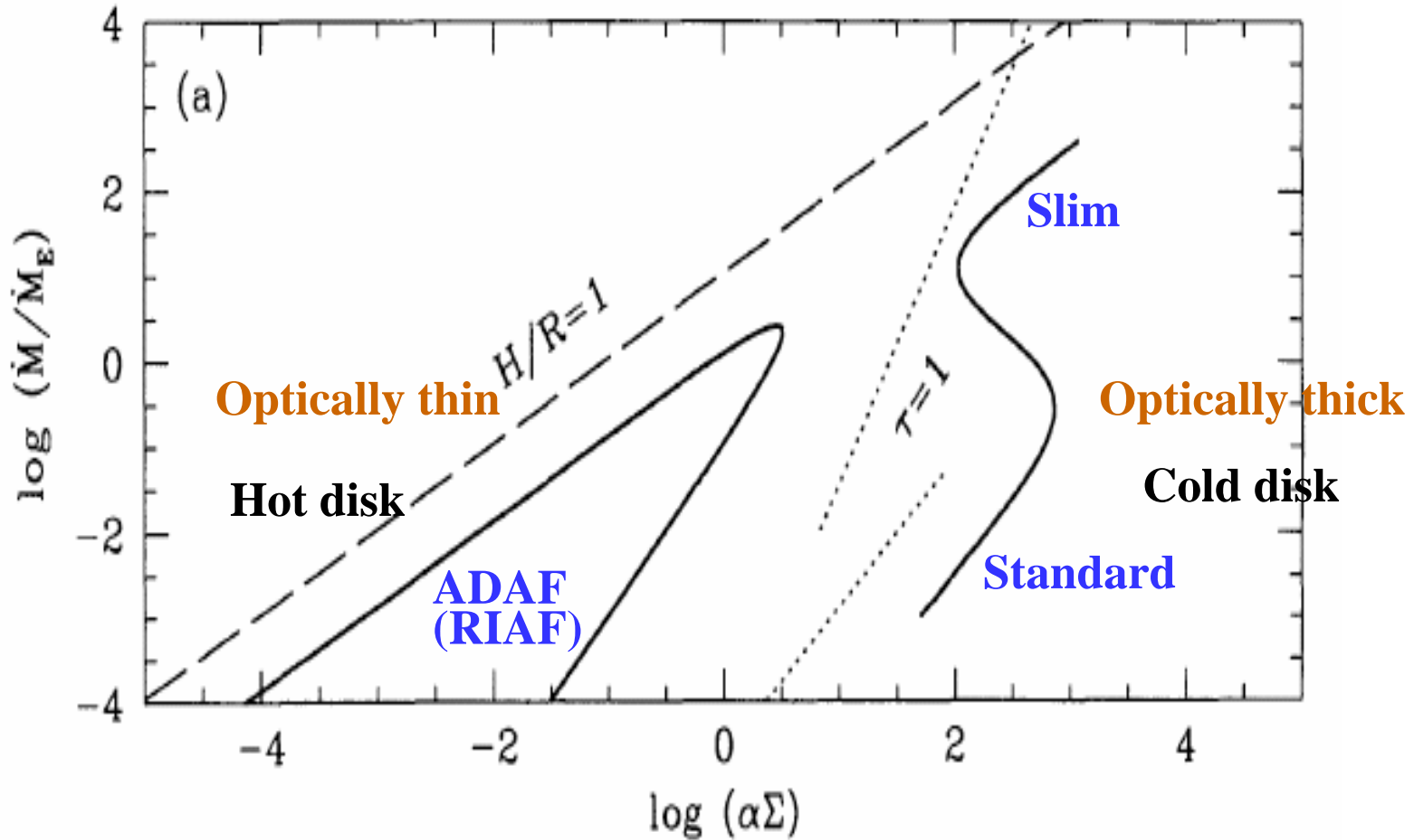
分子粘性:  $\alpha \approx 10^{-10}$

乱流粘性(K-H shear 不安定):  $\alpha \approx 10^{-4}$

磁気粘性:  $\alpha \approx 10^{-2} - 1$

# Accretion Flows

Abramowicz et al. 1995



# Accretion Flows

$$L = \eta n \dot{M}_{\text{E}} c^2, \quad \dot{M}_{\text{E}} = 10 L_E / c^2 = 10 \cdot \frac{4\pi G cm_p M}{\sigma_T c^2}$$

**Sub-Eddington:** ADAF (Advection-Dominated Accretion Flow)  
RIAF (Radiatively Inefficient Accretion Flow)

high energy photons (strong X-ray)

$$\dot{n} \equiv \frac{\dot{M}}{\dot{M}_{\text{E}}} = 1 \Rightarrow \eta \approx 0.1 \dot{n}$$

**Eddington:** Standard Disk

low energy photons

$$\dot{n} \equiv \frac{\dot{M}}{\dot{M}_{\text{E}}} \approx 1 \Rightarrow \eta \approx 0.1$$

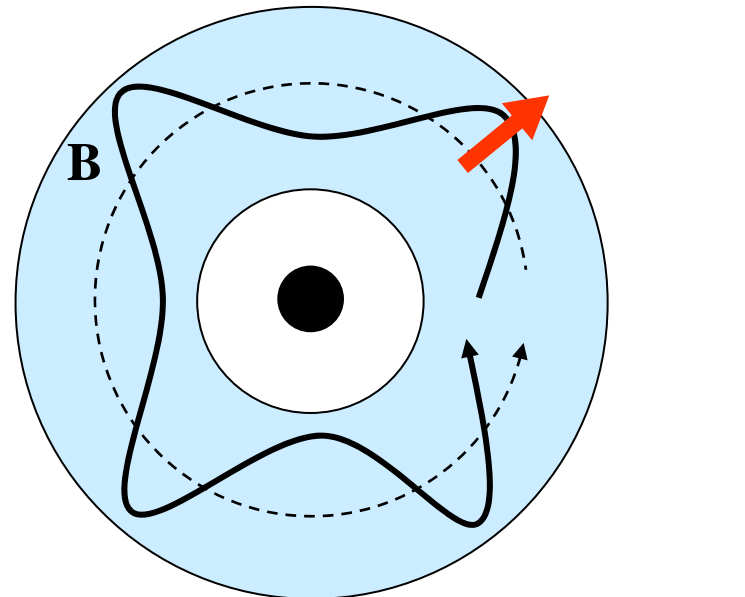
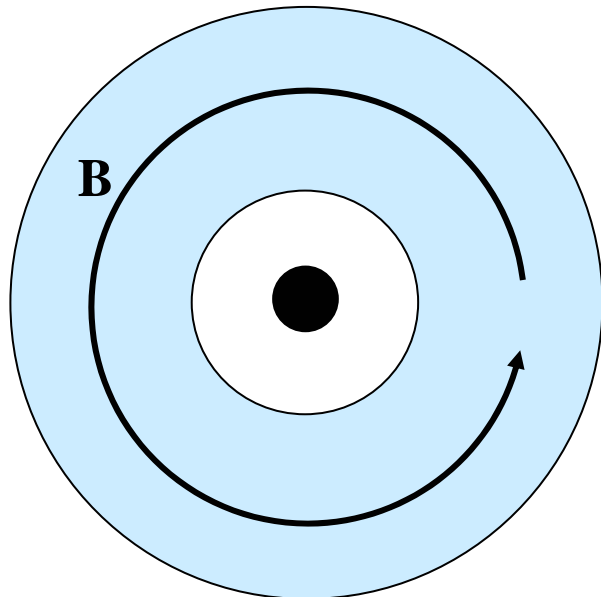
**Super-Eddington:** Slim Disk (Photon trapping)

lower energy photons

$$\dot{n} \equiv \frac{\dot{M}}{\dot{M}_{\text{E}}} > 1 \Rightarrow \eta \approx 0.1 \dot{n}^{-1/2}$$

# MRI (Magneto-Rotational Instability)

(Velinhov 1959, Chandrasekhar 1961, Balbus & Hawley 1991)



$$\text{重力} = \frac{GM\rho}{r^2} \left(1 + 2\frac{dr}{r}\right) \quad \text{遠心力} = (r - dr)\rho\Omega^2 \quad \text{磁気張力} = 2B^2dr \left(\frac{\lambda}{4}\right)^{-2}$$

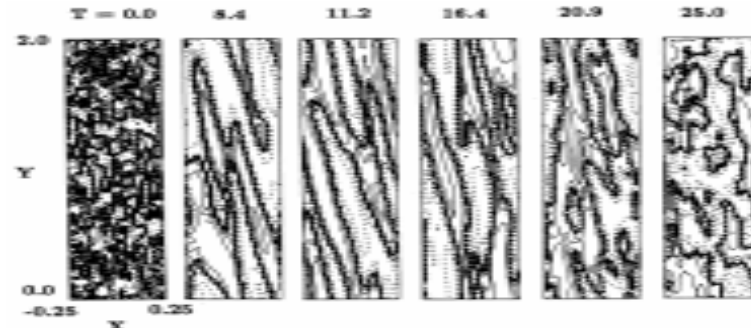
(  $\Omega$  = 一定 )

不安定条件: 重力 + 遠心力 > 磁気張力

$$\lambda > 4\sqrt{\frac{2}{3}}c_A\Omega^{-1} \quad (c_A = \text{Alfven velocity})$$

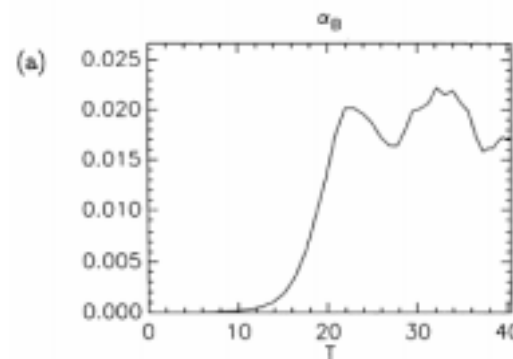
# Magnetic Viscosity

Matsumoto & Tajima 1995, ApJ, 445, 767

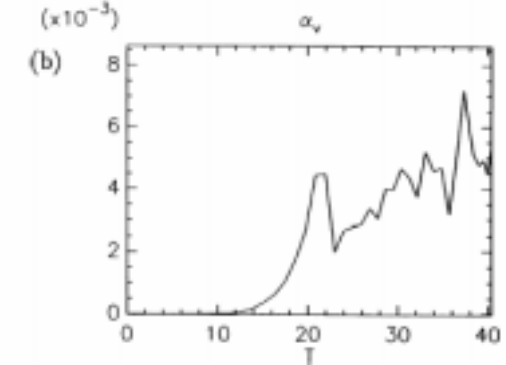


$$\alpha_B = \langle B_x B_y \rangle / 4\pi P$$

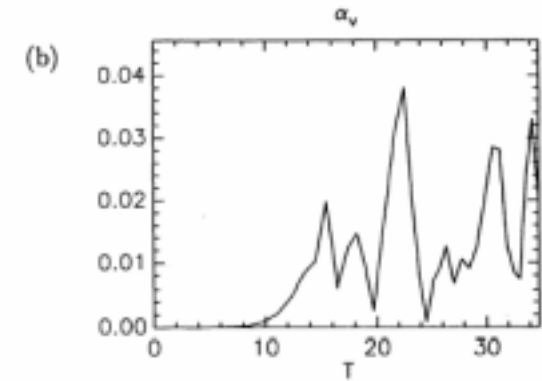
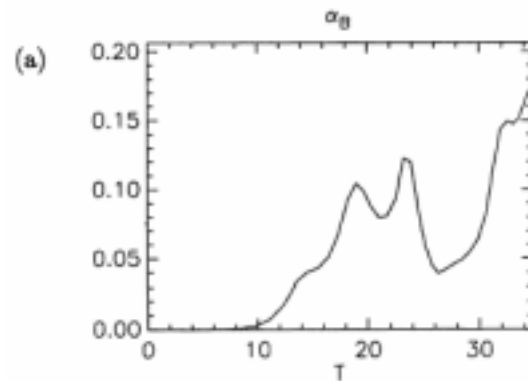
toroidal field model



$$\alpha_V = \rho \langle v_x v_y \rangle / P$$



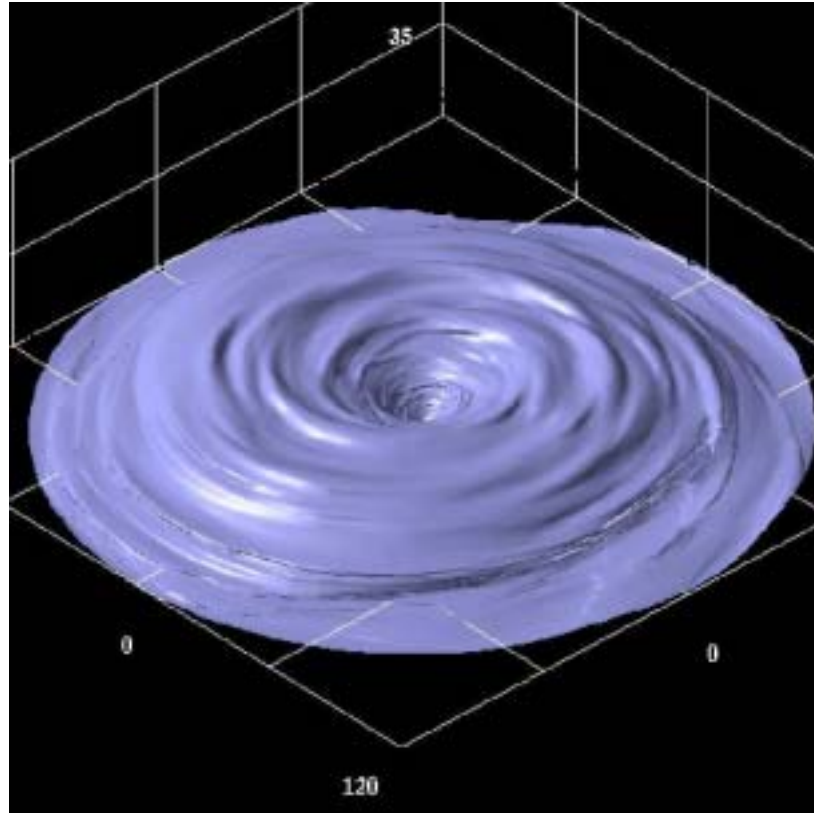
vertical field model



# MHD Simulation of ADAF

Machida, Nakamura, Matsumoto, 2004, PASJ, 56, 671

光学的に薄い accretion flow  
の global structure について MHD 計算



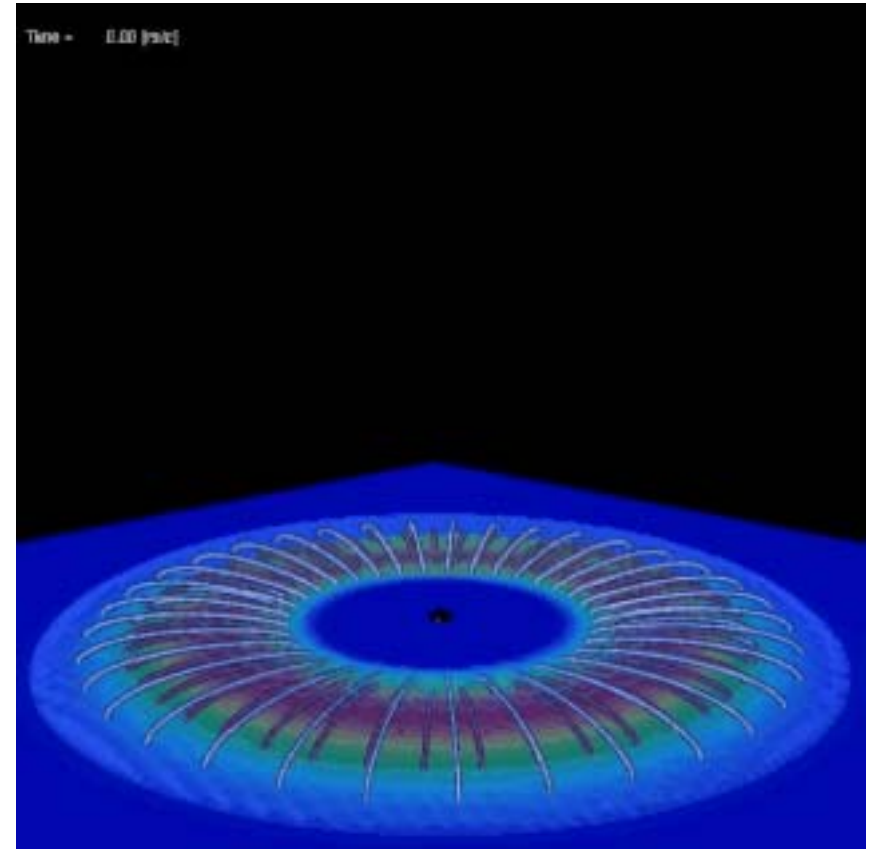
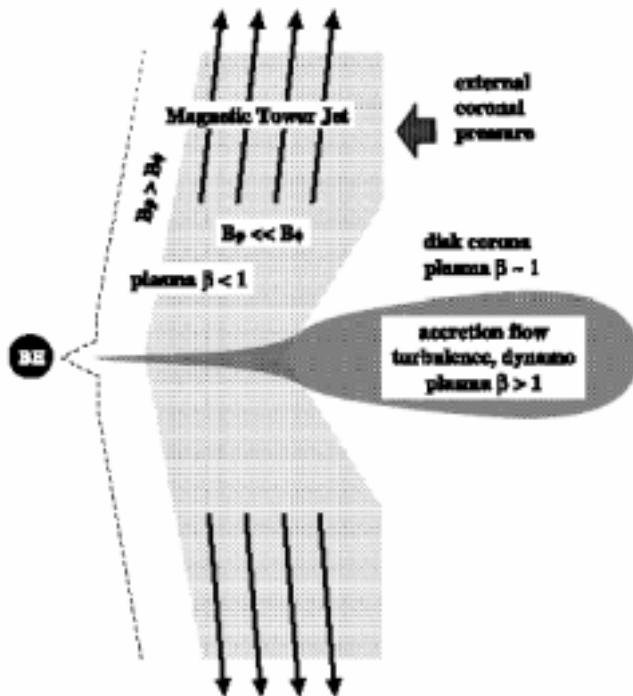
<15 $r_g$  で, optically-thin  
hot disk を形成

||  
ADAF解に一致

# Magnetic-Tower Jet

Lynden-Bell, 1996, MNRAS, 279, 389

Kato, Mineshige, Shibata, 2004, ApJ, 605, 307

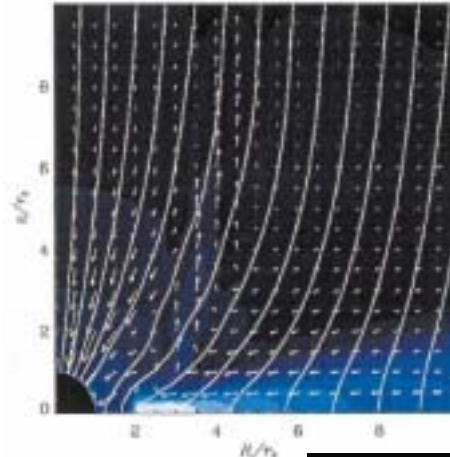
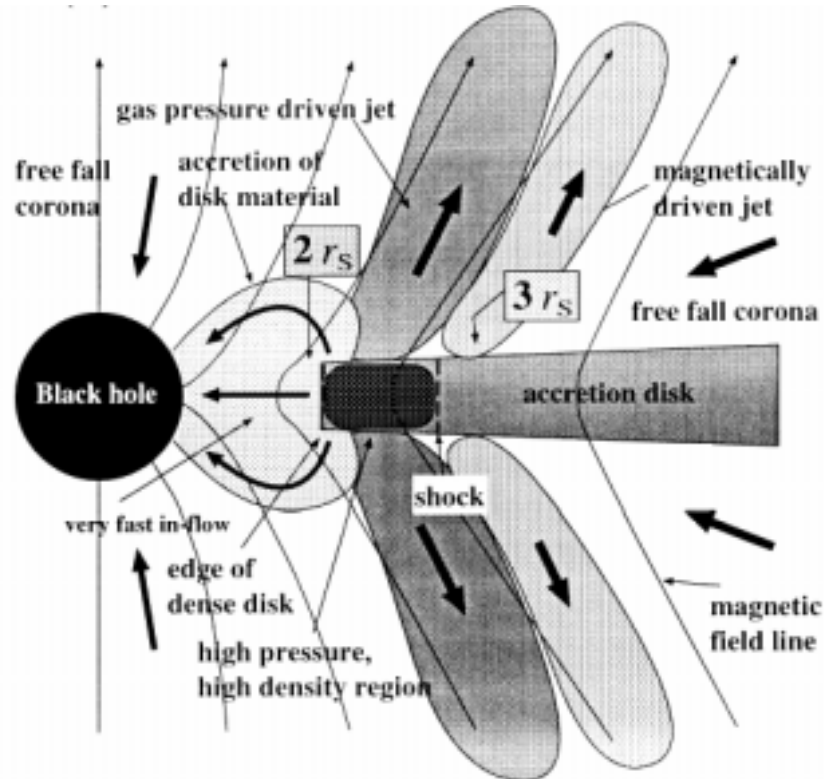


MRI 強いトロイダル磁場形成と浮上  
磁気タワー形成  
磁気圧によりジェット加速 ( $\approx 0.5c$ )

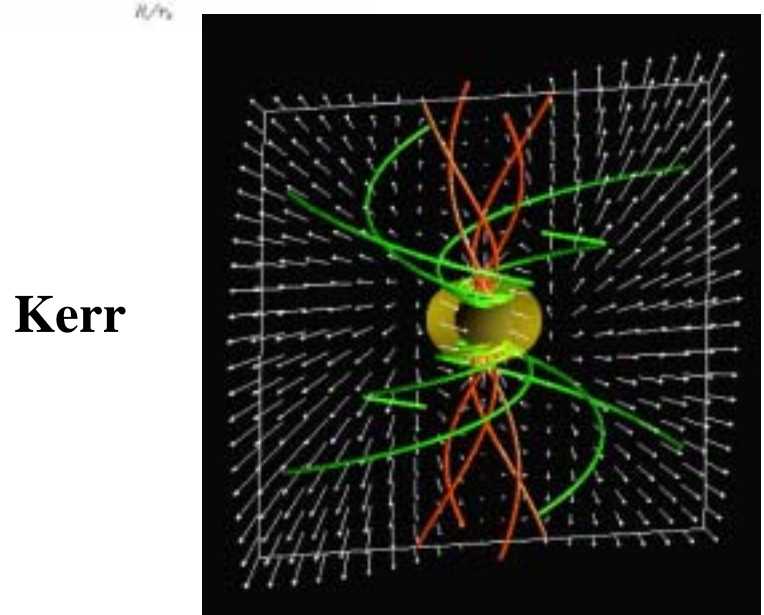
Y. Kato et al. 2004

# GR-MHD

Koide, Shibata, Kudoh, 1999, ApJ, 522, 727 (Schwartzshild)  
Koide, 2004, ApJ, 606, L45 (Kerr)



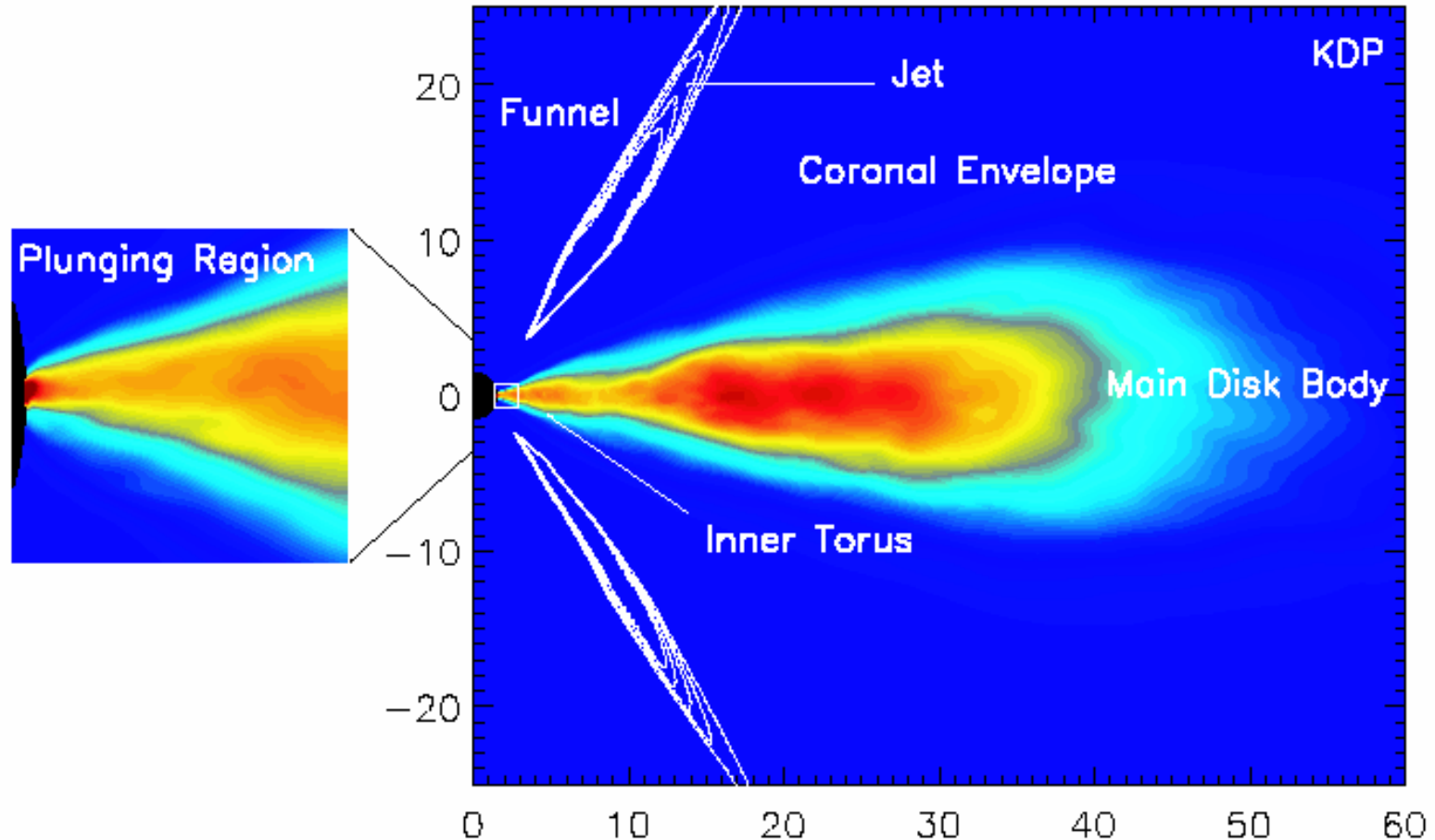
Schwarzschild



Kerr

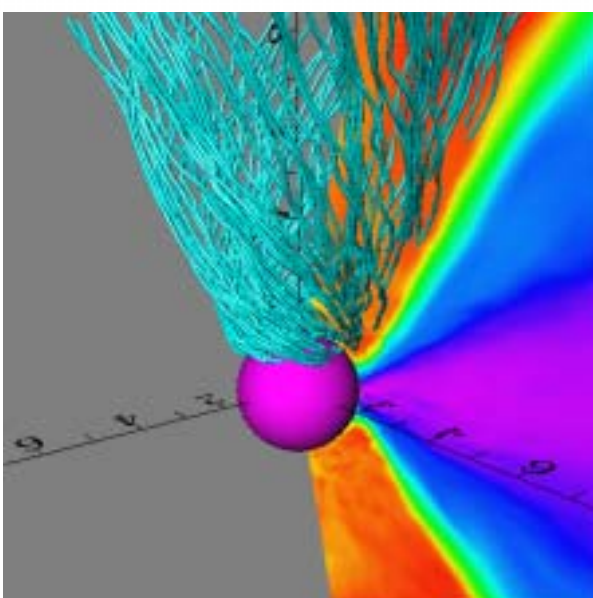
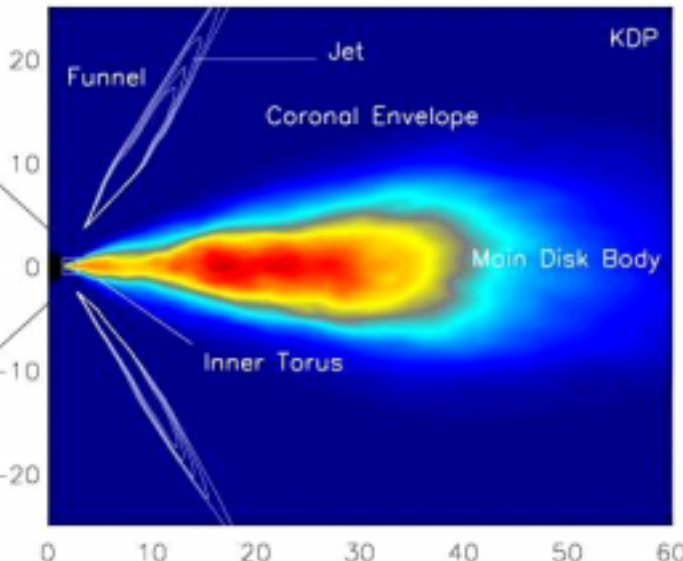
# Accretion Flow around Kerr BH

De Villiers et al. 2003, ApJ, 599, 1238



# MHD Jet around Kerr BH

Hawley & Krolik 2006, ApJ, 641, 103



BH spin によって Toroidal 磁場が生成  
外向きの Poynting flux  
funnel wall に沿って out-flow を生成  
~0.4 - 0.6 c

BH spin が上がると outflow 増大

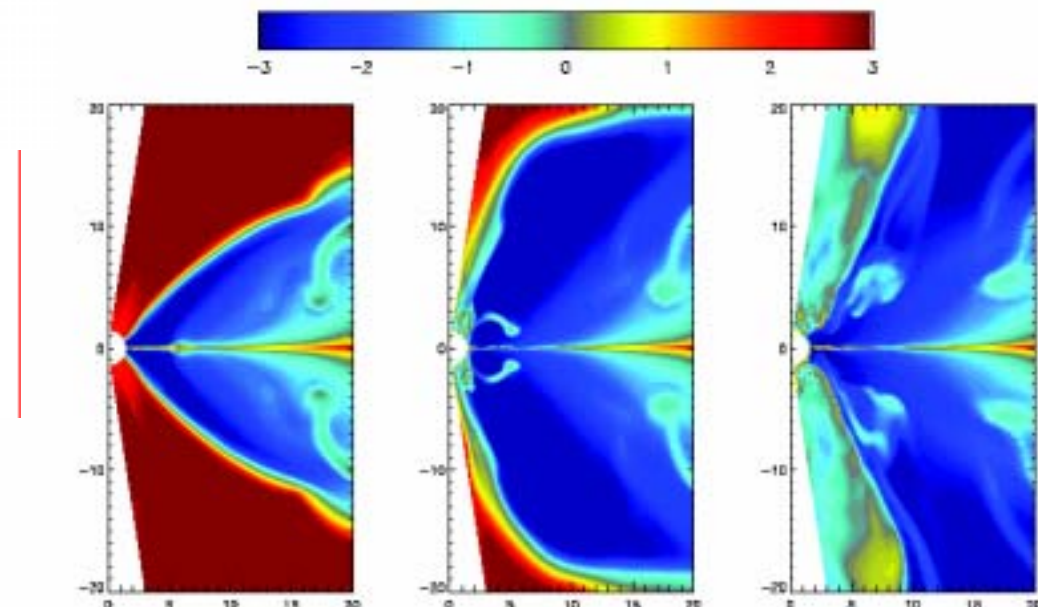


Fig. 2.—Ratio of the azimuthally averaged gas to magnetic pressure ( $\beta$ ) at  $t = 560M$ ,  $640M$ , and  $720M$  in KDPg. The color contours are in a logarithmic scale: dark red is gas pressure-dominated ( $\beta = 10^3$ ) and dark blue is magnetic field-dominated ( $\beta = 0.001$ ).

# Supercritical Accretion

- 高赤方偏移ケーラーからの要請

(Haiman 2004, astro-ph/0403225)

SDSS QSO  $z=6.4$ ,  $M_{\text{BH}} \approx 10^9 M_{\odot}$

$$t_{\text{growth}} ; 7 \times 10^8 \eta_{0.1} \text{ yr}$$

$$t_{\text{H}} ; 9 \times 10^8 \text{ yr at } z=6$$

$$\Rightarrow r \& \equiv \frac{M}{M_{\text{E}}} > 1$$

- Narrow Line Sy 1 & Narrow Line QSOs

(Kawaguchi et al. 2004, A&A, 420, 23L)

$< 10^8 M_{\odot}$  のBH成長は, Super-Eddington

# Slim Disk Model for NLS1

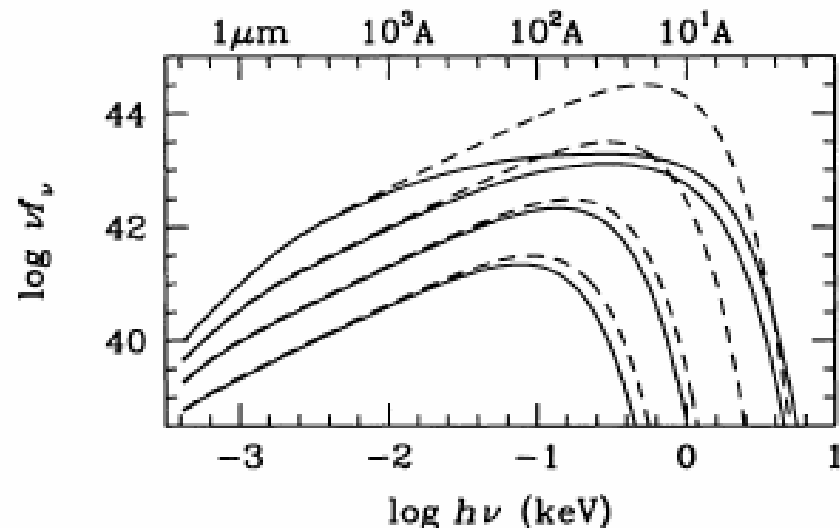
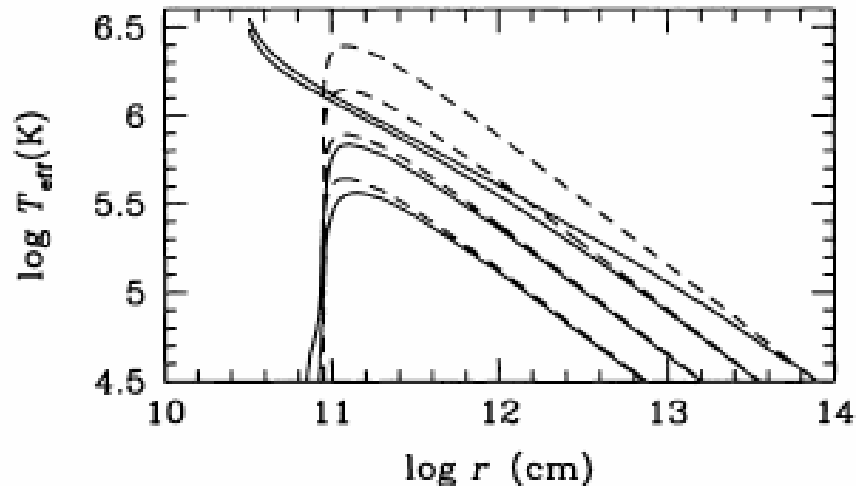
Mineshige et al. 2000, PASJ, 52, 499

## Multi-color spectra

NLS1の観測は

$$n_e^8 > 10$$

で説明できる



# Photon Trapping in Supercritical Accretion

**mass accretion:**  $t_{acc} = r / v_r, \dot{M} = 2\pi r v_r \Sigma$

**photon diffusion:**  $t_{diff} = h / (c / 3\tau), \tau = \sigma_T \Sigma / 2m_p$

**photon trapping condition:**  $t_{acc} < t_{diff}$

$$\left( \frac{\dot{M}}{\dot{M}_E} \right) > 2 \left( \frac{r}{3r_s} \right) \left( \frac{h}{r} \right)^{-1}$$

Supercritical accretion では, photon trapping が起こる  
Outflow  $\Rightarrow$  BH accretion rate はどこまで上がるか



大須賀氏講演

# Accretion Disk & Jet

## 課題

- 磁気粘性ディスクとスペクトル
- 磁場の回転と, BHスピンで, どの程度の angular momentum と mass が outflow で運ばれるか
- BH mass accretion rate は, どこまで大きくなれるか



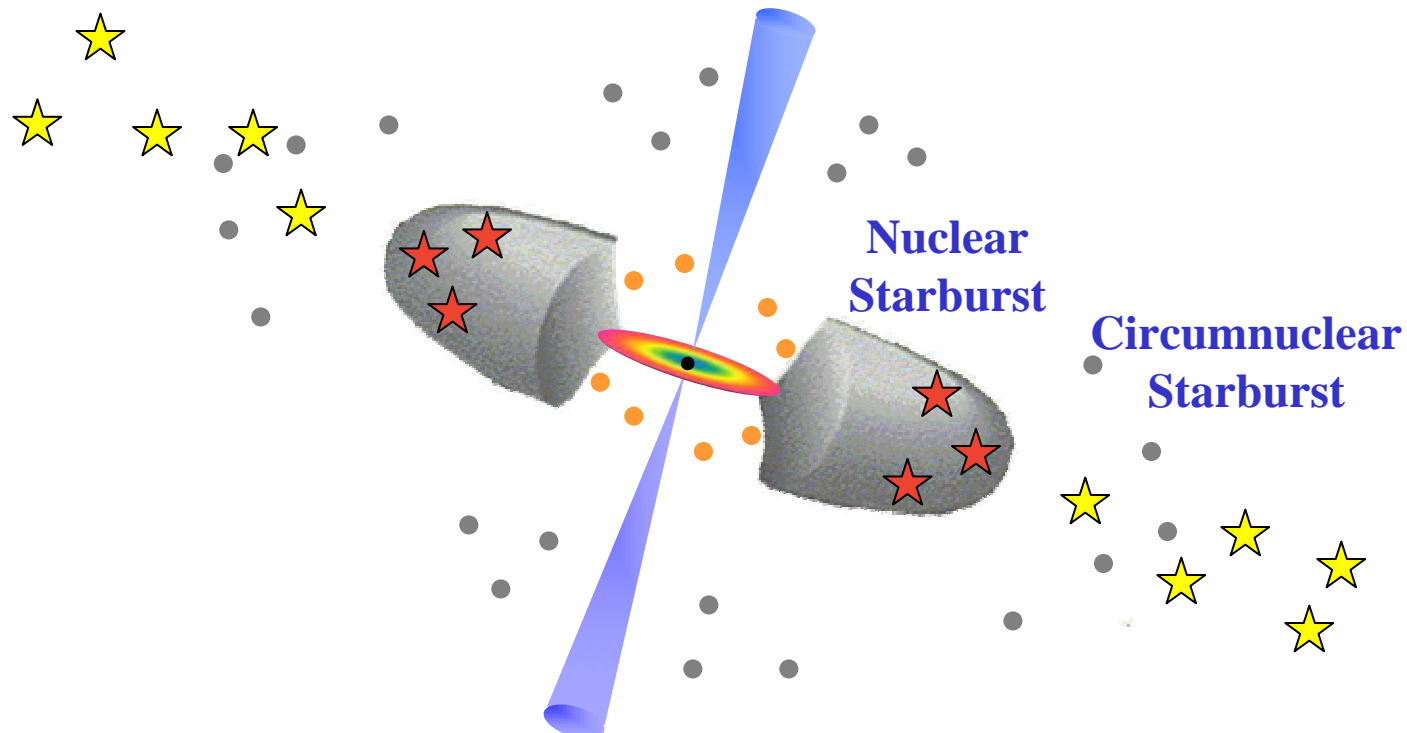
RMHD (Radiation Magneto-Hydrodynamics) が必要

## Part 3 遮蔽とAGNタイプ

# AGN-Starburst Connection

Circumnuclear Starburst (数10pc-1kpc) は2型に多い  
Nuclear Starburst (1-10pc) は1型 , 2型にあまりよらない  
(Hidden Starburst)

単純なトーラスモデルでは説明がつかない！



# Starburst Rings

NGC1300

Barred Spiral Galaxy NGC 1300



# NGC6782

Galaxy NGC 6782



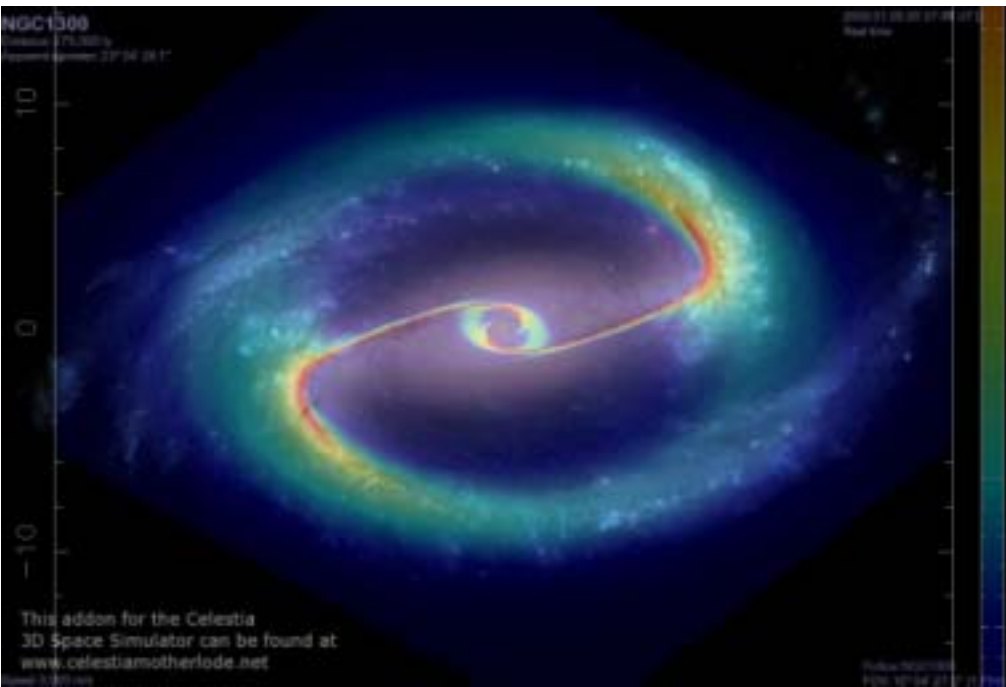
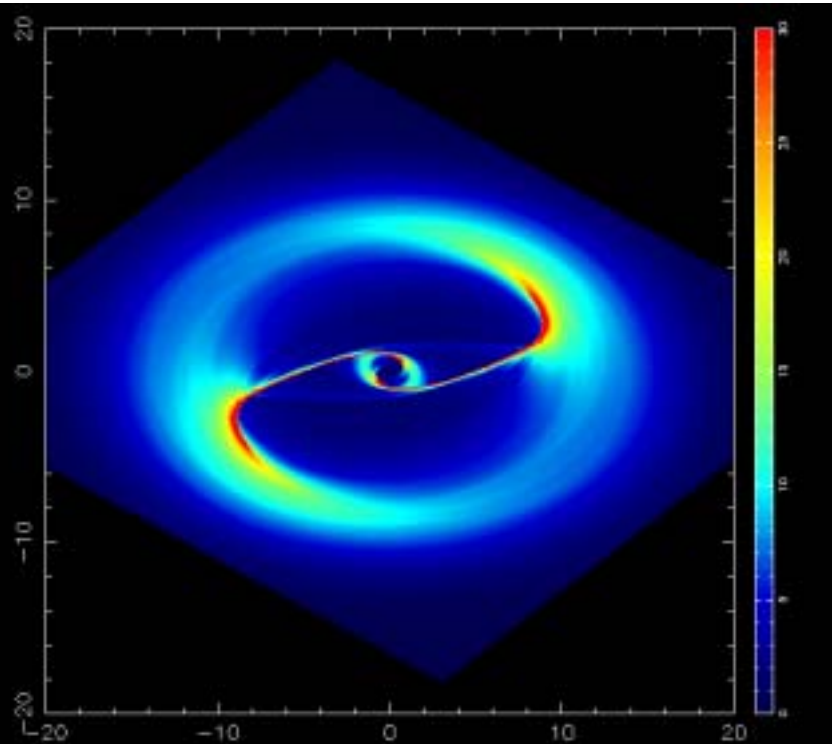
Hubble  
Heritage

# NGC1300

Yen et al 2006

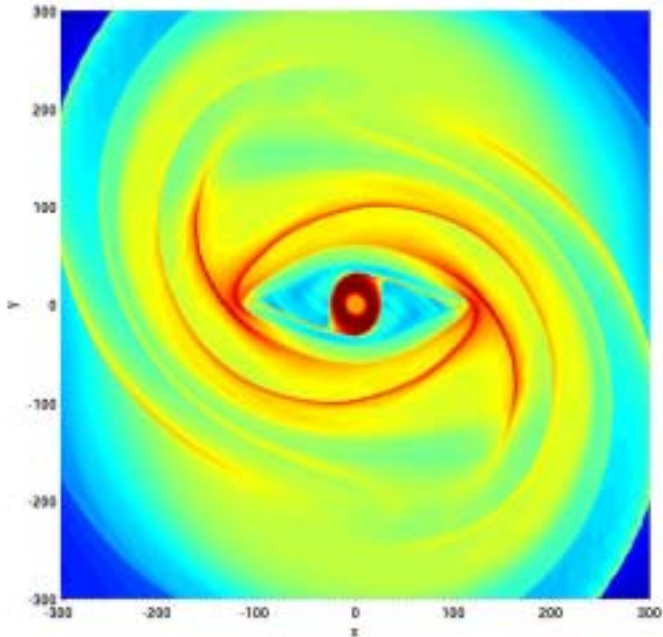
OILR=8.62kpc

$$\Omega_p = 4.1 \text{ km/s} \cdot \text{kpc}$$

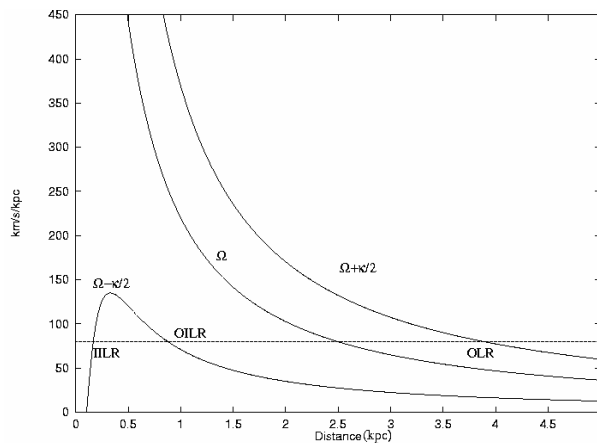


# Double Ring Feature

Yen et al 2006



OLR & OILR



# Turbulent-Supported Obscuring Torus

Wada & Norman, 2002, ApJ, 566, L21

SN feedback による遮蔽トーラス形成と乱流粘性発生

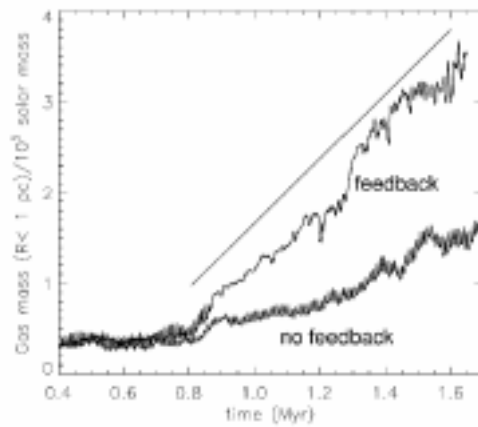
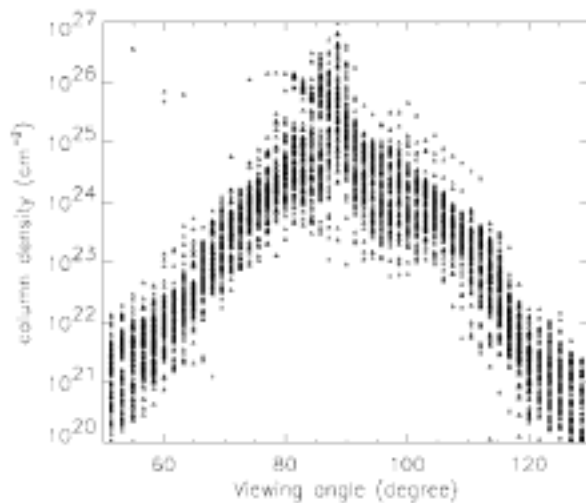
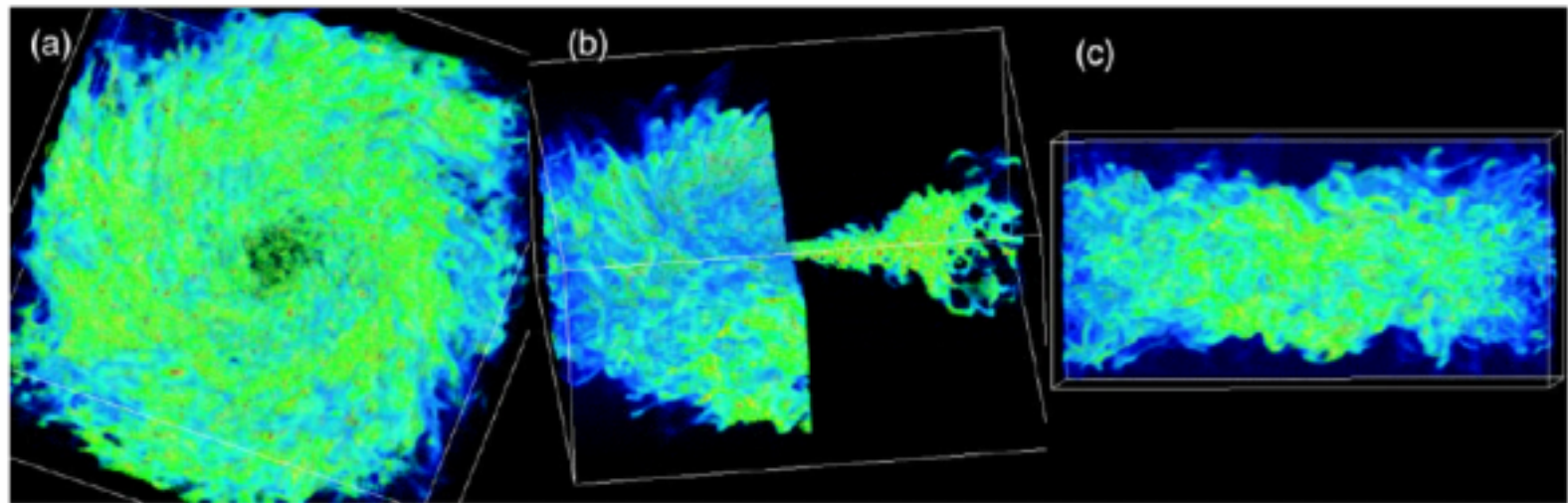
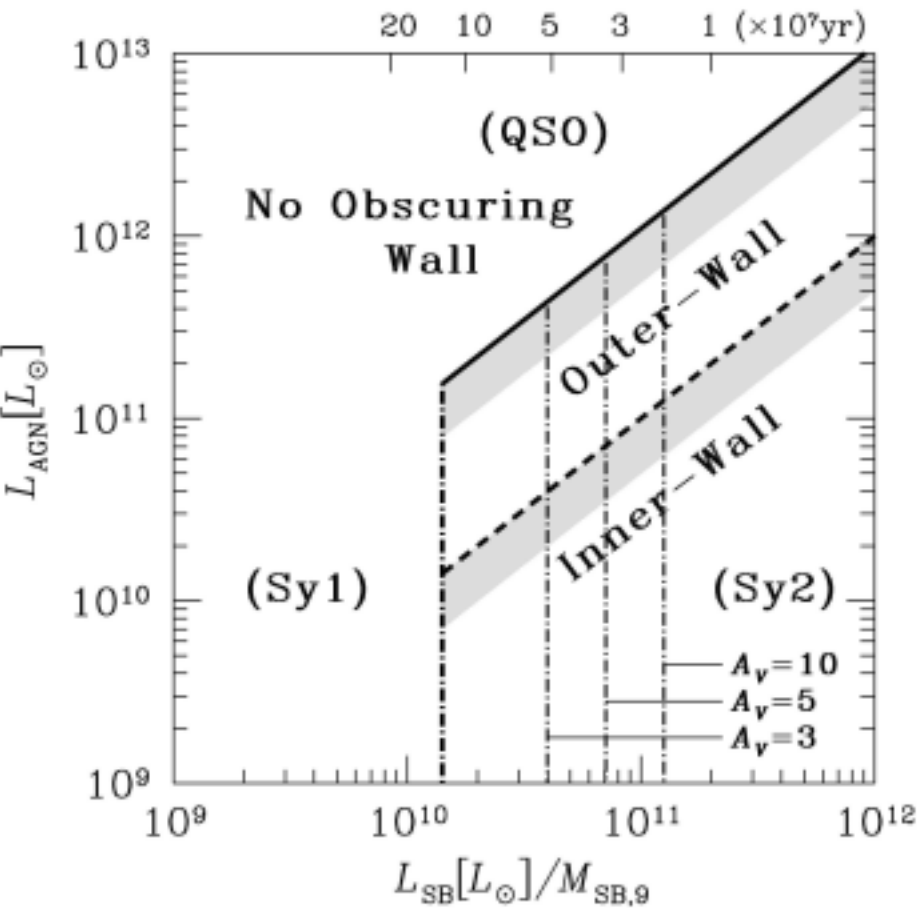
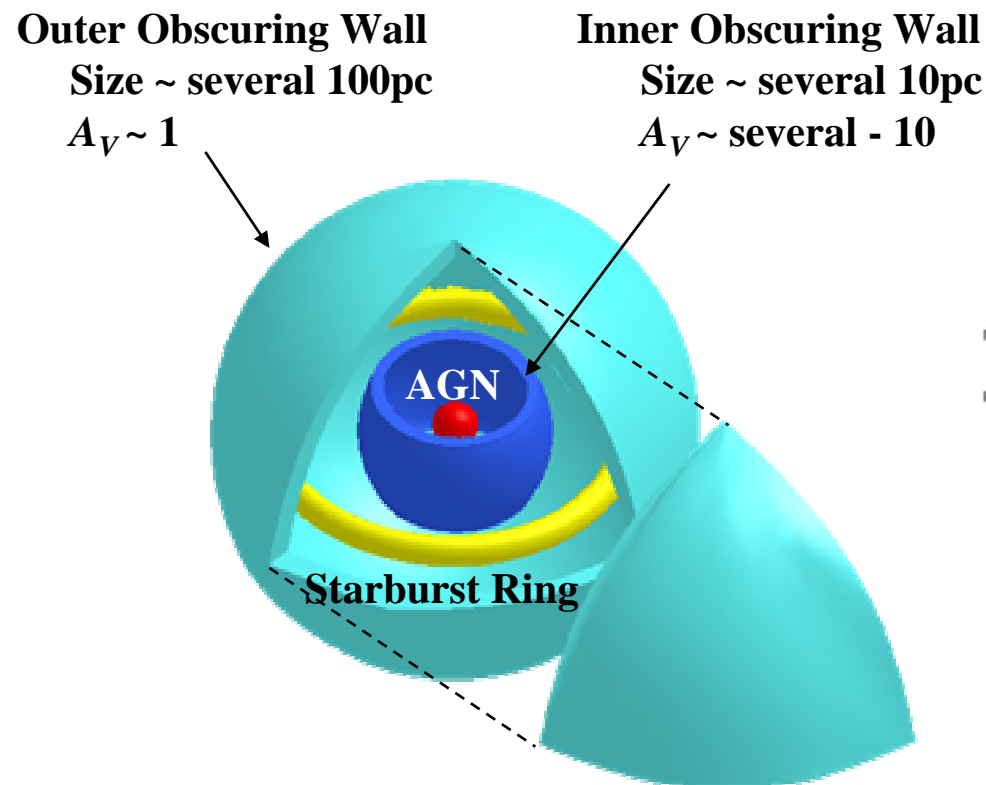


Fig. 3.—Time evolution of the gas mass inside  $R < 1$  pc for two models (with and without energy feedback). Solid line represents the mass accretion rate  $0.3 M_{\odot} \text{ yr}^{-1}$ .

# Obscuring Wall Model

Ohsuga & MU, 2001, ApJ, 559, 157

スタークマントの輻射圧で形成される Stable Gas Wall  
AGNが明るくなると平衡解はなくなる (QSO)

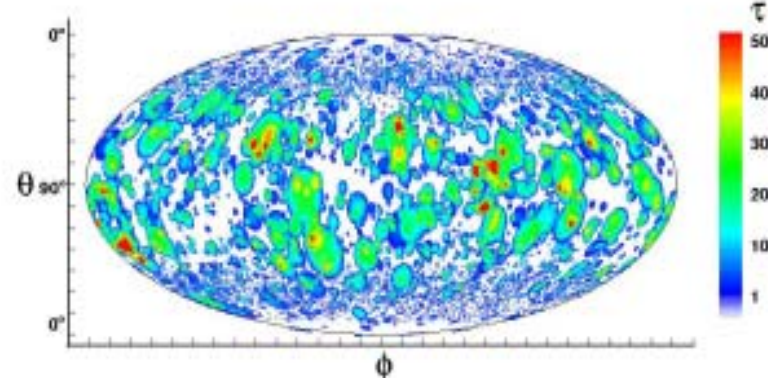
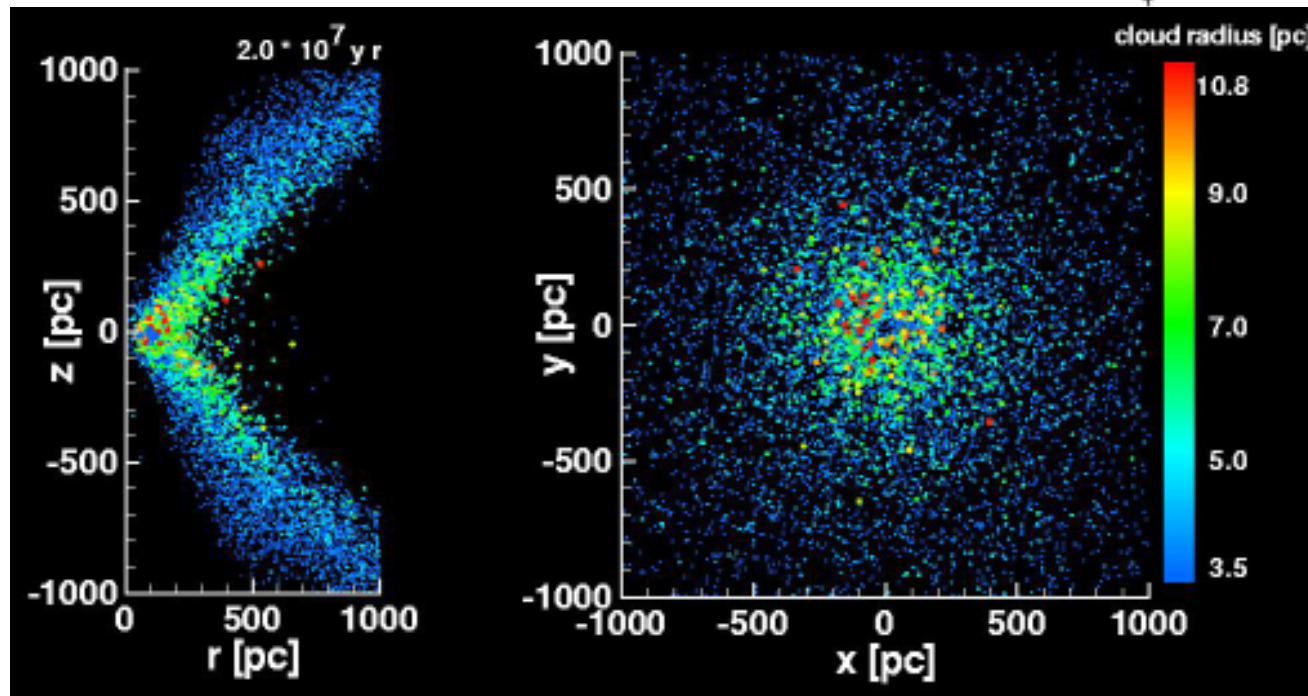


# Radiation-Pressure Driven Obscuring Clouds

Watabe & MU, 2005, ApJ, 618, 649

スターバースト輻射圧によるガス雲の  
巻上げと非一様遮蔽構造発生

$$A_V \sim 1-50$$



# 遮蔽 & AGNタイプ

## 課題

- スターバーストとAGN遮蔽，AGN活動の関係は？
- 観測
  - 可視光  $A_V \sim 1-10$
  - X線  $A_V \sim 100$
  - 遮蔽は一元論でよいか
- ブラックホール降着とどのように関係しているか

# Conclusions

## 超巨大ブラックホール

key physics はかなりわかってきた

銀河スケールからサブパーセックまでつながったわけではない

## 降着円盤 & ジェット

磁気粘性降着円盤のモデルが確立しつつある

輻射の役割はまだ十分にわかっていない

## 遮蔽&AGNタイプ

単純なトーラスモデルは行き詰まっている(?)

スターバーストとの関係

ブラックホールへの降着との関係

**END**